Author for correspondence:
Marc-Thorsten Hütt
e-mail: m.huett@jacobs-university.de

THE ROYAL SOCIETY
PUBLISHING

Two classes of functional connectivity in dynamical processes in networks

Venetia Voutsa[1], Demian Battaglia[2,3], Louise J. Bracken[5], Andrea Brovelli[4], Julia Costescu[5], Mario Díaz Muñoz[6], Brian D. Fath[7,8,9], Andrea Funk[10,11], Mel Guirro[5], Thomas Hein[10,11], Christian Kerschner[6,9], Christian Kimmich[9,12], Vinicius Lima[2,4], Arnaud Messé[13], Anthony J. Parsons[5], John Perez[5], Ronald Pöppl[15], Christina Prell[14], Sonia Recinos[10], Yanhua Shi[9], Shubham Tiwari[5], Laura Turnbull[5], John Wainwright[5], Harald Waxenecker[9] and Marc-Thorsten Hütt[1]

[1]Department of Life Sciences and Chemistry, Jacobs University Bremen, 28759 Bremen, Germany
[2]Aix-Marseille Université, Inserm, Institut de Neurosciences des Systèmes (UMR 1106), Marseille, France
[3]University of Strasbourg Institute for Advanced Studies (USIAS), Strasbourg 67083, France
[4]Aix-Marseille Université, CNRS, Institut de Neurosciences de la Timone (UMR 7289), Marseille, France
[5]Department of Geography, Durham University, Durham DH1 3LE, UK
[6]Department of Sustainability, Governance and Methods, Modul University Vienna, 1190 Vienna, Austria
[7]Department of Biological Sciences, Towson University, Towson, Maryland 21252, USA
[8]Advancing Systems Analysis Program, International Institute for Applied Systems Analysis, Laxenburg 2361, Austria
[9]Department of Environmental Studies, Masaryk University, 60200 Brno, Czech Republic
[10]Institute of Hydrobiology and Aquatic Ecosystem Management (IHG), University of Natural Resources and Life Sciences Vienna (BOKU), 1180 Vienna, Austria
[11]WasserCluster Lunz - Biologische Station GmbH, Dr. Carl Kupelwieser Promenade 5, 3293 Lunz am See, Austria
[12]Regional Science and Environmental Research, Institute for Advanced Studies, 1080 Vienna, Austria
[13]Department of Computational Neuroscience, University Medical Center Eppendorf, Hamburg University, Germany
[14]Department of Cultural Geography, University of Groningen, 9747 AD, Groningen, The Netherlands
[15]Department of Geography and Regional Research, University of Vienna, Universitätsstr. 7, 1010 Vienna, Austria

VV, 0000-0001-6079-0292; MG, 0000-0003-1565-5686; TH, 0000-0002-7767-4607; AM, 0000-0001-9081-3088; YS, 0000-0001-7575-6177; LT, 0000-0002-3307-1214; M-TH, 0000-0003-2221-423X

The relationship between network structure and dynamics is one of the most extensively investigated problems in the theory of complex systems of recent years. Understanding this relationship is of relevance to a range of disciplines—from neuroscience to geomorphology. A major strategy of investigating this relationship is the quantitative comparison of a representation of network architecture (structural connectivity, SC) with a (network) representation of the dynamics (functional connectivity, FC). Here, we show that one can distinguish two classes of functional connectivity—one based on simultaneous activity (co-activity) of nodes, the other based on sequential activity of nodes. We delineate these two classes in different categories of dynamical processes—excitations, regular and chaotic oscillators—and provide examples for SC/FC correlations of both classes in each of these models. We expand the theoretical view of the SC/FC relationships, with conceptual instances of the SC and the two classes of FC for various application scenarios in geomorphology, ecology, systems biology, neuroscience and socio-ecological systems. Seeing the organisation of dynamical processes in a network either as governed by co-activity or by sequential activity allows us to bring some order in the myriad of observations relating structure and function of complex networks.

1. Introduction

The relationship between network structure and dynamics has been at the forefront of investigation in the field of complex systems during the past decades, with networks serving as powerful abstract representations of real-world systems. However, a solid theoretical understanding of the generic features relating network structure and dynamics is still missing. Here, our strategy of investigating these features is via the quantitative comparison of network architecture (structural connectivity, SC) with a network (or matrix) representation of the dynamics (functional connectivity, FC). We establish key relationships using simple model representations of dynamics: excitable dynamics represented by a stochastic cellular automaton, coupled phase oscillators, chaotic oscillators represented by coupled logistic maps. We validate these relationships in coupled FitzHugh-Nagumo oscillators, in the excitable and the oscillatory regimes. Furthermore, we give examples of how the two classes of FC can be applied to various application domains, in which networks play a prominent role.

The simplest way of representing time series of dynamical elements as a network is to compute pairwise correlations. Often, one also knows about the 'true' or 'static' connectivity of these dynamical elements beforehand. The statistical question then arises in a natural way, whether the known network (SC) and the network derived from the dynamical observations (FC) are similar. As we will see in the applications, functional connectivity can either be thought of as dynamical similarities of nodes or flows (of material, activity, information, etc.) connecting two nodes.

The simplicity of the dynamics included in our investigation allows us to work with this correlation-based approach. In case of a large heterogeneity of dynamical elements, very noisy dynamics, poor statistics (temporal sampling) or incomplete information, more sophisticated representations of dynamical relationships among nodes are required [1–5].

Originating in neuroscience [6], research into SC/FC correlations has become a promising marker for changes in systemic function and a means for exploring the principles underlying the relationship between network architecture and dynamics—in systems biology [7,8], social sciences [9–11], geomorphology [12–14] and technology [15–17], just to name a few of the application areas.

Such SC/FC relationships are at the same time markers for certain forms of systemic behaviour (e.g. a loss of SC/FC correlation may indicate pathological brain activity patterns [18]) and highly informative starting points for a mechanistic understanding of the system (e.g. revealing highly connected elements—hubs—as centres of self-organized excitation waves in scale-free graphs [19,20]).

While the systemic implications and the key results have been reviewed elsewhere [21], here we would like to show that across a range of dynamical processes and network architectures some fundamental common principles exist. We argue that one needs to distinguish between two types of functional connectivity, one related to synchronous activity (or co-activation), the other related to chains of events (or sequential activation). A system, like phase oscillators [22–24], favouring one type of functional connectivity (for this example, synchronization) can also display the other type of SC/FC correlations under certain conditions.

A condition here is characterized by the network type, the strength of the coupling of the dynamical elements and the choice of further (intrinsic) parameters of each of the dynamical elements. Here, we show many examples of transitions from one type of SC/FC correlations to another type under changes of these conditions.

Stylized models of dynamics often offer a deep mechanistic understanding of the dynamical processes and phenomena and, in particular, help discern how network architecture shapes the dynamical behaviour. This point is illustrated by the intense research over the past decades on networks of coupled phase oscillators as a stylized model of oscillatory dynamics. Two prominent examples of this line of investigation are the topological determinants of synchronizability [23,25], the lifetimes of intermediate synchronization patterns in a time course towards full synchronization and their relationships to the network's modular organization [22].

Remarkably, it is precisely this formal distinction between functional connectivity based on co-activation and sequential activation that is often hard to discriminate in more detailed (e.g. continuous) models [26] and experimental data [27].

In the case of SC/FC correlations, the best-investigated stylized model is the—three-state cellular automaton—SER model of excitable dynamics [19,28,29]. Key results include that the topological overlap [30] is highly associated with functional connectivity based on simultaneous activity, FC_{sim}, and that via this mechanism—a clustering of high topological overlap values within modules—modular graphs display high SC/FC correlations, while scale-free graphs tend to display low, or even systematically negative SC/FC correlations with this definition of FC [28,30]. Furthermore, a large asymmetry of the sequential activation matrix (which is the foundation of functional connectivity based on sequential activation, FC_{seq}) can be associated with self-organized waves around hubs [20]. Additionally the role of cycles for organizing SC/FC correlations has been investigated [31] and in the deterministic limit of the model, a theoretical framework for predicting SC/FC correlations has been established [30].

As a first illustration of the tremendous power of probing networks with various types of dynamics, in order to understand how network architecture determines some of the dynamical features, in figure 1, we show snapshots of dynamical states for three real-life networks coming from different domains—Neuroscience (the macaque cortical area network from [32]), systems biology (the core metabolic system of the gut bacterium *Escherichia coli* from [33]) and social sciences (intra-organizational network of skills awareness in a company from [34])—under the action of three types of dynamics—excitable dynamics, phase oscillators, the logistic map as an example of a chaotic oscillator.

The real-life networks shown in figure 1 can all be considered examples of structural connectivity. The detailed description of the structure of these networks is given in the electronic supplementary material.

An important question around figure 1 is whether the three types of dynamics are plausible for the networks at hand. First, we would like to emphasize that the strategy of our investigation is to probe network architectures by simple prototypes (or very stylized forms) of dynamics, rather than devising realistic models of the most plausible form of dynamics for each of these networks.

In the case of the cortical area network, the excitable dynamics as well as the oscillatory dynamics can be seen as stylized but plausible dynamical probes and, in fact, those have been previously employed to explore such network
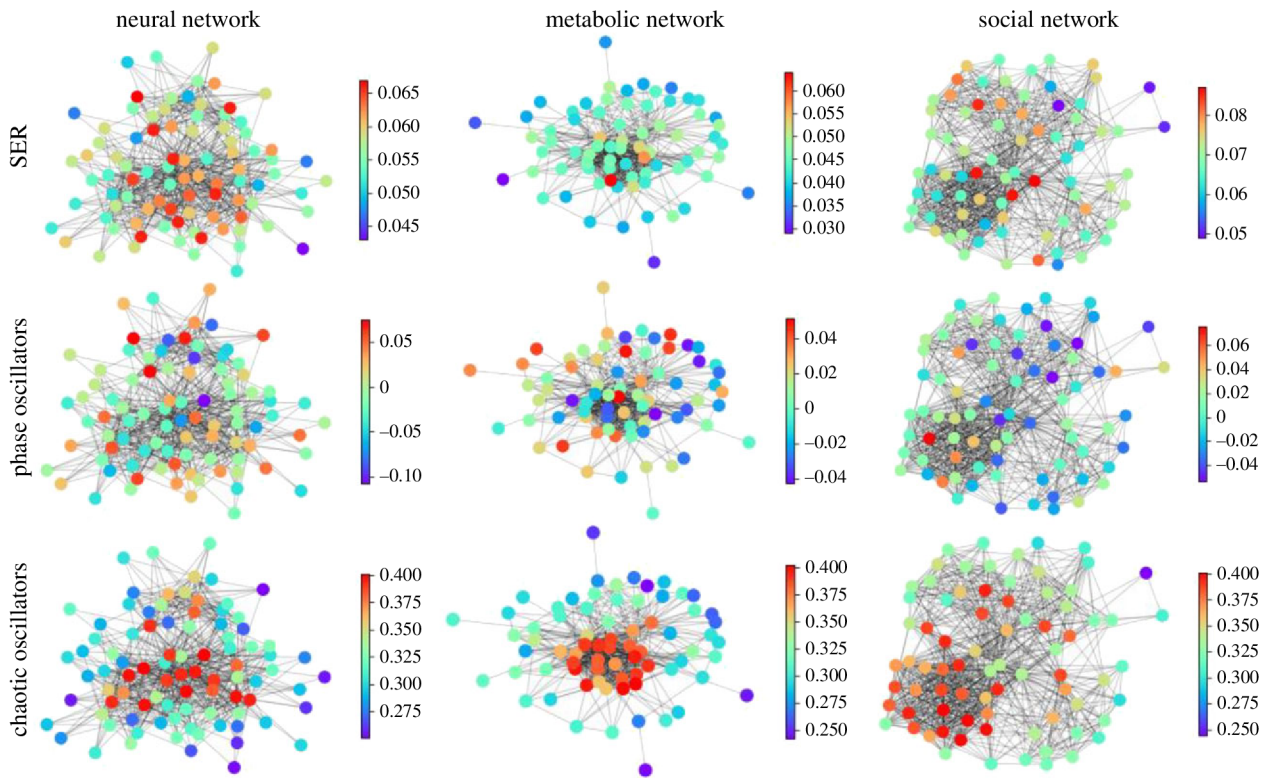
Figure 1. An illustrative example of applying different categories of dynamical processes to real networks with different structures. Neural network: macaque cortical area network from [32]. Metabolic network: core metabolic system of the gut bacterium *Escherichia coli* from [33]. Social network: skills awareness network from [34]. SER: The mean activity of each node after 1000 timesteps, with a rate of spontaneous activity $f = 0.001$ and a recovery probability $p = 0.1$. Phase oscillators: The average effective frequency of each node for ten simulations of length $T = 200$ initialized with a uniform distribution of eigenfrequencies. Logistic map: The average standard deviation of the time series of each node for 10 simulations of 500 timesteps with the parameter R for each node randomly selected from a uniform distribution with $R_{min} = 3.7$ and $R_{max} = 3.9$.

structures [20,35–37]. But also chaotic dynamics, as in the third row of figure 1, have been used to study neuronal connectivity patterns [38,39].

In the case of metabolic networks, synchronous activity patterns, and hence coupled phase oscillators, are a plausible form of dynamics (see, for example, the arguments in [40], where enzymes are described as cyclically operating devices, as well as the prominent usage of correlation networks in metabolomics [41–43]). A more pathway-oriented view of metabolism might emphasize the propagation of activity and, hence, would be closer to the excitable dynamics shown in the first row of figure 1. Chaotic oscillators are clearly less relevant for this application domain.

Interaction dynamics, contact dynamics and information flow in a corporate setting unite aspects of excitable dynamics (as in the case of rumour spreading, [44]) or synchronization [45,46]. But also chaotic dynamics have been employed to model decision dynamics and activity in corporate settings [47–49].

The three main messages of the illustration of dynamics on real-life networks shown in figure 1 are: (1) The representation of complex systems as networks enables the probing of such complex structures with dynamics. (2) Different networks react differently to one type of dynamics. This general point can be seen for example in figure 1 by following one type of dynamics (e.g. excitable dynamics; first row in figure 1) across the three networks and observing that groups of nodes acting together (similar colour, representing similar dynamical states) can be either in the periphery or in the centre of these network representations. (3) A given network reacts differently

to different dynamical probes. This general feature can be seen by following a single network across different types of dynamics (columns in figure 1). Regions in the graph with a similar dynamical state (same colours) for one dynamics look heterogeneous (different colours) for another dynamics. Also, similarities occur. The periphery and the centre of the networks tend to behave differently in all the examples of dynamics shown in figure 1.

It is obvious that such an illustration can only provide a single snapshot of the diverse dynamics possible on such networks, even for a single type of dynamics, as the internal parameters at each node, as well as the coupling type and strength among them can have different values. In the following, we want to further explore the systematic changes of these dynamical patterns as a function of network architecture, coupling and internal dynamical parameters and how this theoretical framework can be applied to various disciplines.

2. Results and discussion

We create different instances that indicate the behaviour of the two classes of FC using various numerical schemes. The means of enhancing or destroying SC/FC correlations can be structural (i.e. driven by network architecture) or dynamical (induced by changing the parameters of the dynamical model). The investigation is organized around the form of change: §2.1 topological changes, §2.2 changes in the coupling strength, §2.3 changes of the intrinsic parameters of the individual elements. In §2.4, we illustrate these principles in a case
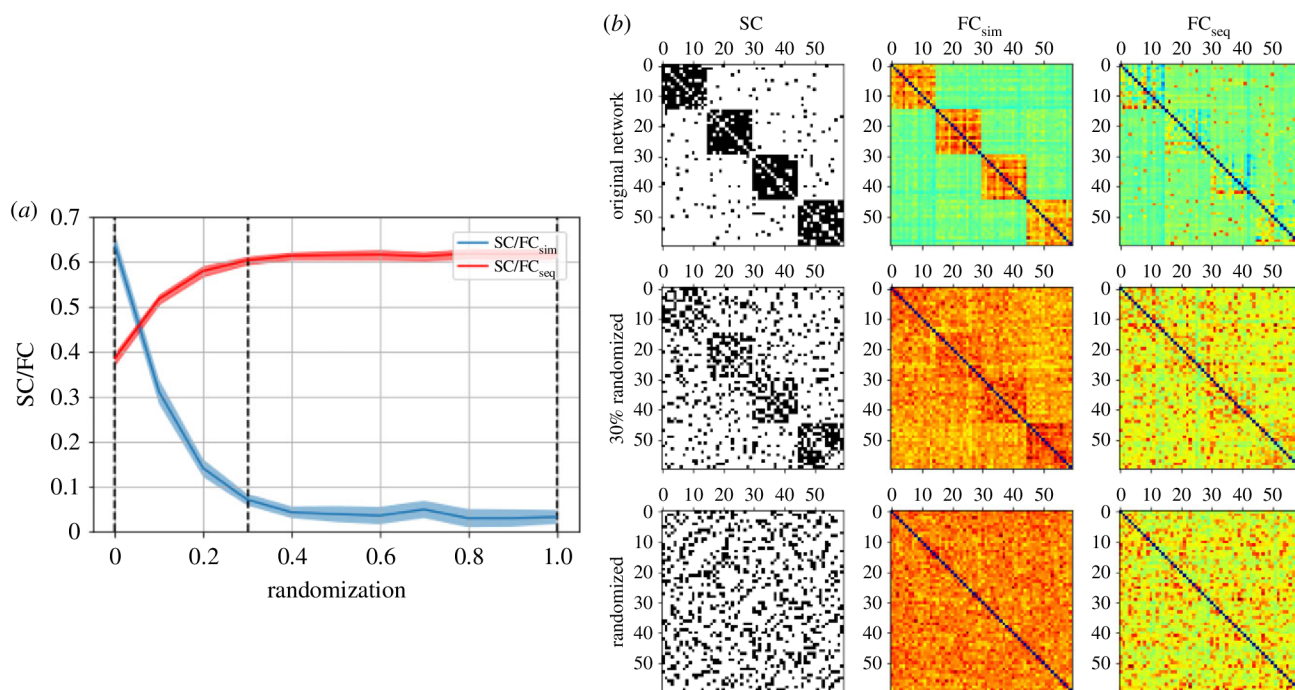
Figure 2. (*a*) SC/FC$_{sim}$ and SC/FC$_{seq}$ correlations across the randomization of a modular network. (*b*) Illustration of the SC and the FC$_{sim}$, FC$_{seq}$ matrices for three network cases, pointed out by the dashed vertical black lines on the left figure (original modular network, 30% randomized network and completely randomized network). The dynamical model used for the FC is the SER model (parameters: $t_{max} = 10$, $N_R = 10000$, $p = 0.1$, $f = 0.001$.)

study on a network of coupled FitzHugh–Nagumo oscillators in the excitable and oscillatory regimes. Using the three examples from figure 1, in §2.5, we show the behaviour of SC/FC correlations on these real-world networks.

2.1. Topological changes

The first part of our investigation is related to the effect of topology in the SC/FC correlations. We started with networks with a distinct structure (modular graph, hierarchical graph, regular graph), which we gradually destroyed either by randomizing or by rewiring the initial network (see Methods, §5).

Figure 2 introduces the comparison of structural connectivity and functional connectivity on the matrix level, by depicting the adjacency matrices of two networks, together with examples of the corresponding functional connectivity matrices derived from dynamics (here: the co-activation and sequential activation matrices obtained from simulations of the SER model; see Methods, §5). This matrix view on SC/FC relationships is similar to fig. 1 in [26] and fig. 1 in [28] and allows us to visually discern the strong positive correlation between the adjacency matrix and the co-activation matrix in the case of the modular graph (first row) and the apparent lack thereof in the more random graph (second row), for which we, however, can visually perceive an agreement between the adjacency matrix and the sequential activation matrix. So, here a change in network topology goes along with a change from one type of SC/FC correlations (co-activation to sequential activation). This is the phenomenon we set out to explore further in the following.

In the electronic supplementary material, figures S2 and S3 show the same matrix view, but for coupled phase oscillators and logistic maps, respectively. In figure S2 (phase oscillators) in the electronic supplementary material, a visual inspection clearly shows that the SC/FC correlations based on sequential activation are much weaker than the

ones based on co-activation. Also, SC/FC$_{sim}$ remains visibly high during randomization. In figure S3 in the electronic supplementary material (logistic maps), the lack of correlation between co-activation and the modular structure is clearly seen, as is the (faint, but discernible) agreement of this modular structure with sequential activation. Careful visual inspection also reveals the persisting positive SC/FC$_{seq}$ correlations, as well as the negative SC/FC$_{sim}$ correlations, under randomization of the modular network. In figure S4 in the electronic supplementary material examples of space–time plots for single runs of the chaotic dynamics are shown and this thus provides a microscopic view of the results summarized in figure 2.

In figure 3, we go from rather structured network topologies to rather unstructured random network topologies. Figure 3 supports the visual impression from the matrix examples shown in figure 2 by showing the two types of SC/FC correlations as a function of network randomization procedures, for the SER model (which was also used in figure 2), as well as two other types of dynamics, namely coupled phase oscillators and coupled logistic maps in the chaotic regime (see Methods, §5). It should be noted that each of these dynamical models has been instrumental in the past in advancing our understanding of fundamental relationships between network architecture and dynamics (see, e.g. [19,30,50] for the SER model, [22,24] for coupled phase oscillators, and [51,52] for the logistic maps).

For the SER model, we see a trend that structured topologies favour high SC/FC correlations of both types, whereas unstructured random networks favour high SC/FC$_{seq}$ correlations. We can also see that SC/FC$_{sim}$ is very sensitive to topological changes, in contrast to SC/FC$_{seq}$, which, in this case, shows a more stable behaviour. The networks of coupled phase oscillators behave in almost the opposite way, where co-activation (rather than sequential activation) is favoured by random network structures and shows a more stable
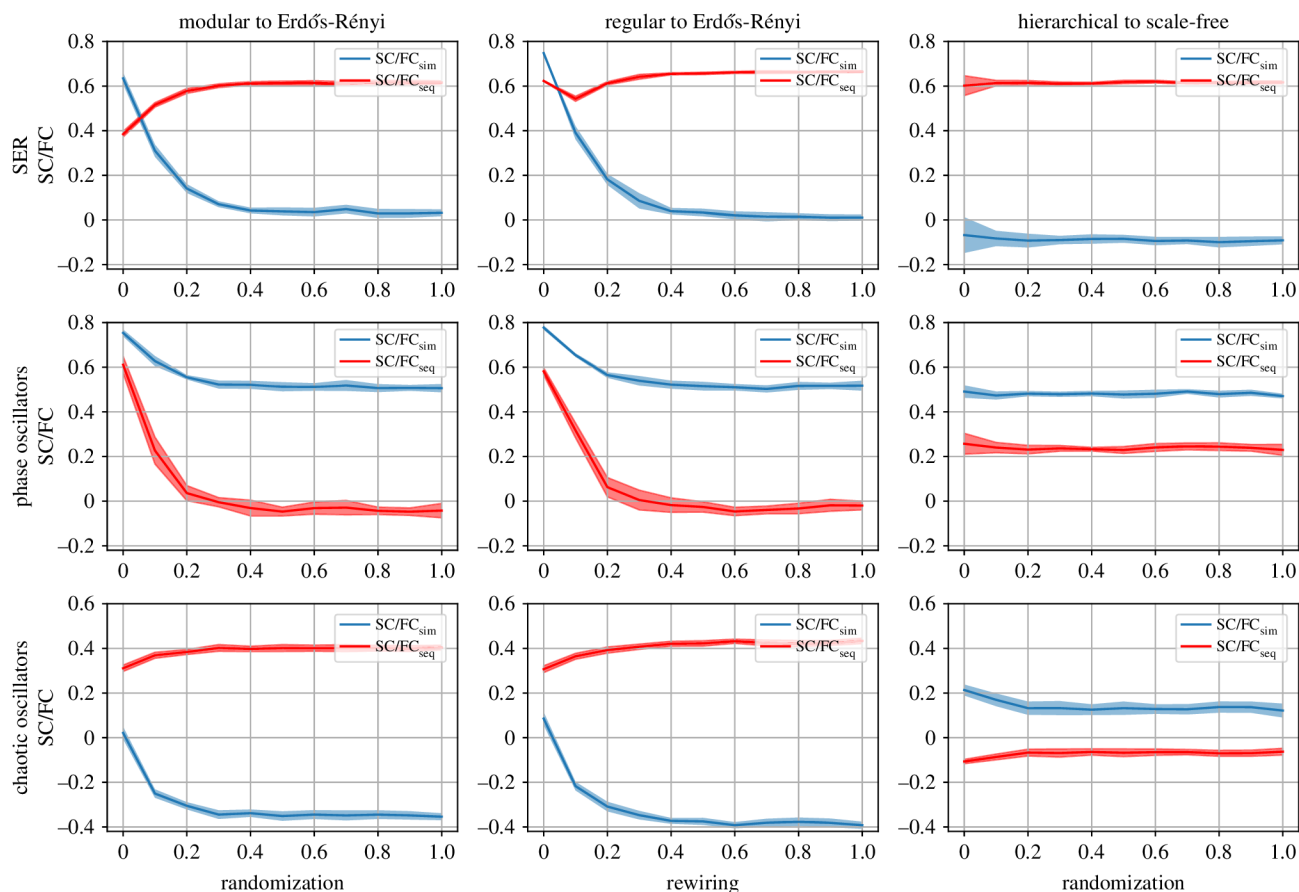
Figure 3. SC/FC$_{sim}$ and SC/FC$_{seq}$ correlations across the range of randomization/rewiring processes. First column: randomization of a modular graph. Second column: rewiring of a regular graph. Third column: randomization of a hierarchical graph in the three models. First row: SER model; parameters: $t_{max} = 10$, N_R (over different initial conditions) = 10 000, N_R (over different initial graphs) = 10, $p = 0.1$, $f = 0.001$. Second row: coupled phase oscillators; parameters: $t_{max} = 50$, N_R (over different initial conditions) = 100, N_R (over different initial graphs) = 10, $\omega \in (0, 1)$, $k = 10$, $\sigma = 0.25$, $u \in (0, 1)$. Third row: logistic map (chaotic oscillators); parameters: $t_{max} = 500$, N_R (over different initial conditions) = 50, $R \in (3.7, 3.9)$, $k = 2$.

behaviour under topological changes. In the case of chaotic oscillators, the details about the network architecture and the selection of the type of coupling matter. For this case, the transition from structured to unstructured networks does not affect the SC/FC$_{seq}$, but leads to strong negative correlations of the SC/FC$_{sim}$. The hierarchical network is the only one, though, in which the destruction of the modularity is not revealed from the dynamics. For this graph, all the dynamical models show that the randomization does not essentially affect the value of SC/FC correlations, instead constant, low positive correlations of SC/FC$_{seq}$ and constant, low negative correlations of SC/FC$_{sim}$ are maintained during the randomization process.

2.2. Changes in coupling strength

The second set of our numerical experiments pertains to changes in the coupling strength among nodes. For this type of change, only the models of the phase and chaotic oscillators can be used, as the SER model—in the form used here—has no coupling parameter (which could, however, be introduced via a relative excitation threshold, as in [29,53]).

Figure 4 shows that in the case of coupled phase oscillators, all the network architectures stabilize SC/FC$_{sim}$ against changes of coupling strength. Large values of coupling strength lead to rapid synchronization (co-activity of the nodes) and therefore to inadequate amount of information for the sequential activation. As a result, seeing the structure

of the network through the dynamics using the sequential activation is, in this case, not possible. For the chaotic oscillators, we observe general trends of increasing SC/FC$_{seq}$ with increasing coupling, reaching a maximum, and gradually decreasing for further increase of the coupling, essentially across all network architectures (figure 4).

2.3. Changes in intrinsic parameters

Each dynamical model is characterized by specific intrinsic parameters that determine the behaviour of the individual elements and of the system, too. Changes in the values of the intrinsic parameters may result in drastic changes to the functional connectivity. In this part of the investigation, the two types of functional connectivity are studied as a function of such intrinsic parameters. We are here attempting to address the following question: is there at least one class of the functional connectivity that can survive under the changes of a dynamical parameter of the model? Or relatedly, is it possible to observe the structure of the network through the dynamics even if we are consistently changing an intrinsic parameter?

The stochastic SER model is characterized by the recovery probability, p, that determines if a node in the refractory state will return to the susceptible state. For the phase oscillators, we use the range of natural frequencies as the intrinsic parameter. The logistic map has only one intrinsic parameter, R, which defines the dynamical behaviour of the uncoupled
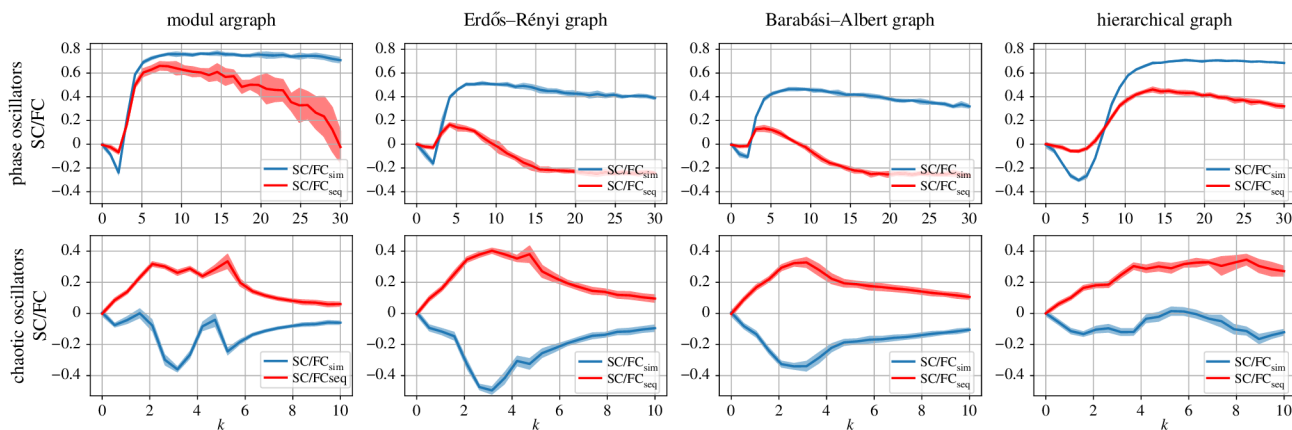
Figure 4. SC/FC$_{sim}$ and SC/FC$_{seq}$ correlations as a function of the coupling strength among the nodes in the two types of oscillators applied to different network architectures. First column: modular graph. Second column: Erdős-Rényi graph. Third column: Barabási-Albert graph. Fourth column: hierarchical graph. First row: coupled phase oscillators; parameters: $t_{max} = 50$, $N_R = 100$ (over different initial conditions), $N_R = 10$ (over different initial graphs), $\omega \in (0, 1)$, $k = 10$, $\sigma = 0.25$, $u \in (0,1)$. Second row: logistic map (chaotic oscillators); parameters: $t_{max} = 500$, $N_R = 50$, $R \in (3.7, 3.9)$, $k = 2$.
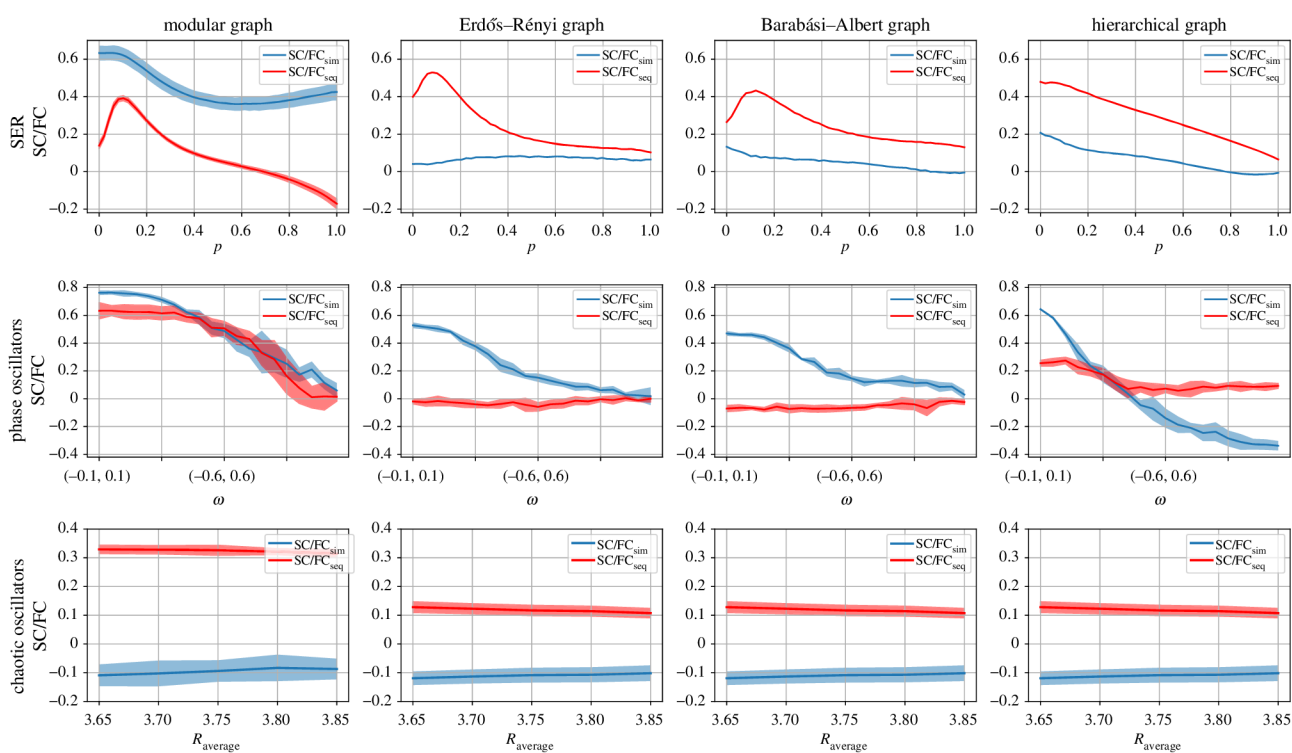
Figure 5. SC/FC$_{sim}$ and SC/FC$_{seq}$ correlations under changes of dynamical parameters in the three models. First row: SER model with increasing recovery probability (parameters: $t_{max} = 10$, $N_R = 10\,000$ (over initial conditions), $N_R = 10$ (over different initial graphs), $f = 0.001$). Second row: coupled phase oscillators under a widening of the distribution of the natural frequencies (parameters: $t_{max} = 50$, $N_R = 100$ (over initial conditions), $N_R = 10$ (over different initial graphs), $k = 10$, $\sigma = 0.25$, $u \in (0, 1)$). Third row: logistic map under a shift of $R_{average}$ of the distribution of R within the interval $(3.7, 3.9)$, keeping the width equal to 0.2 (parameters: $t_{max} = 500$, $N_R = 50$ (over initial conditions), $k = 2$). Four network architectures were used for each model: First column: modular graph. Second column: Erdős-Rényi graph. Third column: Barabási-Albert graph. Fourth column: hierarchical graph.

oscillator. We here vary the average R such that the uncoupled oscillator would reside in the chaotic regime (3.7, 3.9).

Figure 5 shows the results of this part of the investigation. For the SER model, we see that network effects are consistent across the whole parameter range. We can see that SC/FC$_{sim}$ is consistently high for the modular graph and very close to zero for all the other graphs, where, in contrast, the SC/FC$_{seq}$ has positive correlation values. For the phase oscillators, the width of the frequency distribution matters: increasing width leads to a consistent decrease of

SC/FC$_{sim}$, but leaves SC/FC$_{seq}$ intact in all graphs, except for the modular, in which the behaviour of SC/FC$_{seq}$ is similar to SC/FC$_{sim}$. The logistic map does not show any parameter sensitivity of SC/FC correlations in the different network architectures.

2.4. Additional case study

The FitzHugh–Nagumo model can be used as a case study verifying whether our previous results translate to this
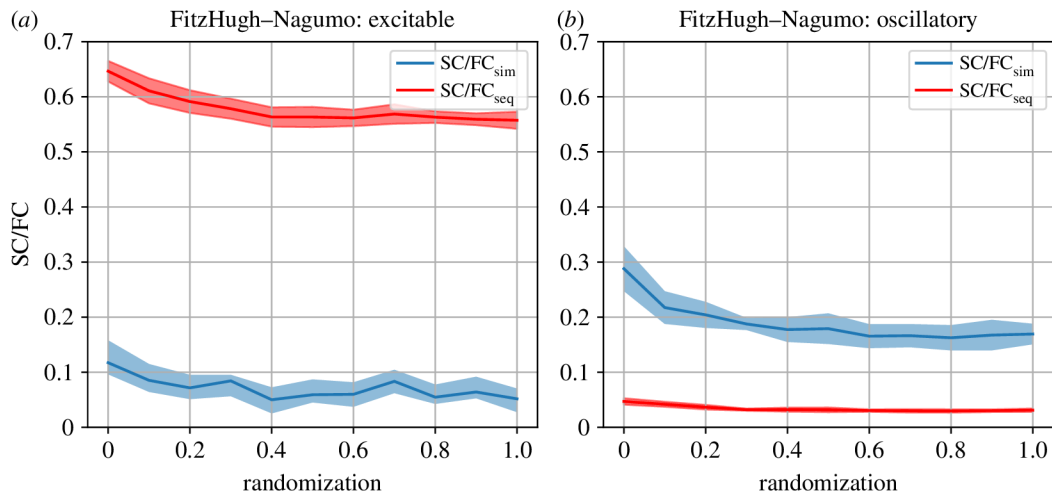
Figure 6. SC/FC correlations from the FitzHugh–Nagumo model in excitable (*a*) and oscillatory (*b*) regime while randomizing random modular networks. The blue curves represent co-activation (i.e. a time window of 1 ms), while the red curves represent sequential activation (i.e. using a time window of 12 ms).

more detailed, more realistic model. To this end, we study the behaviour of SC/FC correlations as a function of randomizing a modular graph in the oscillatory regime ($a = 0$) and in the excitable regime ($a = 0.8$). The results of this more complicated model shown in figure 6 confirm the general observations derived from the two corresponding minimal models: the excitable dynamics enhance the SC/FC_{seq} across the transition of a modular to an Erdős–Rényi graph, whereas oscillations favour the SC/FC_{sim} across the randomization process.

2.5. SC/FC correlations in real networks

We can now return to the real-life networks from figure 1 and study the two types of SC/FC correlations in these networks as a function of the intrinsic parameters of the dynamical models, as done in figure 5 for the abstract network architectures. The results are summarized in figure 7. Regarding the SER model, we see high SC/FC_{seq} correlations for the neural system and, in contrast, high SC/FC_{sim} correlations for the social system, under the increase of the recovery probability, while in the case of the metabolic system, the type of SC/FC correlation that is higher depends strongly on the parameter value. For the phase oscillators, we see initially high correlations that approach zero value as we increase the width of the eigenfrequencies distribution, with the SC/FC_{sim} to have constantly higher values. In the metabolic network, dominant and relatively strong and stable SC/FC_{sim} appears under the same changes of the ω distribution, whereas the zero values of SC/FC_{sim} for the narrow distributions give place to strong negative correlations as we move to wider distributions. The behaviour of the social network is similar to the neural one, but with lower SC/FC correlation values. The results for the logistic map are dominated by SC/FC_{seq} correlations, independent of network architecture and parameter value.

3. Applications

In this section, we briefly review some areas of application to illustrate, (1) how structural connectivity can be defined in these contexts, (2) which approaches for defining functional

connectivity exist in this domain and (3) how the two types of functional connectivity appear in this setting.

Throughout this investigation, we have the following scenario in mind: given a network (structural connectivity) and dynamical processes for each of the nodes, we analyse the time series observed at each node and derive relationships among the nodes (functional connectivity) in order to understand how network architecture determines or shapes the dynamical relationships among nodes. This interplay of structure and dynamics is then illustrated by and quantified in terms of SC/FC correlations. The topic of dynamics on graphs is, of course, much broader than we describe it here. The clear distinction between (static or slowly changing) structural connectivity—which serves as 'infrastructure' for dynamical processes—and (often rapidly changing) functional connectivity is not plausible for all applications. As a consequence, a debate about SC/FC correlations is not possible in important areas of research. Often, in those disciplines, the evolution of the network itself under the action of its agents (nodes) is investigated, therefore we can only conceptualize the FC in the context of the evolution of the structure of the network. Social network analysis (SNA) is the methodology of choice for such situations [54] (see electronic supplementary material for more details).

When multiple relationships must be taken into account to provide a more realistic and precise description of a complex system or when interactions go beyond the pairwise level (with examples from systems biology being protein complexes or biochemical reactions), hypergraphs [55,56] can serve as a useful framework for representing these systems. Furthermore, if the structural network changes on a similar timescale to functional connectivity or even under the influence of the functional dynamics, we enter the rich field of adaptive networks [57–59]. In this case, inevitably, the topology influences the character of the collective dynamics of the system, but dynamics affect topology, too, leading to a continuing interplay between them. This is of particular relevance in social–ecological systems (see §3.5).

3.1. Application to geomorphology

Within hydrology and geomorphology, the examples of structurally connected pathways that we will discuss here are those that direct the flow of water and sediment over the
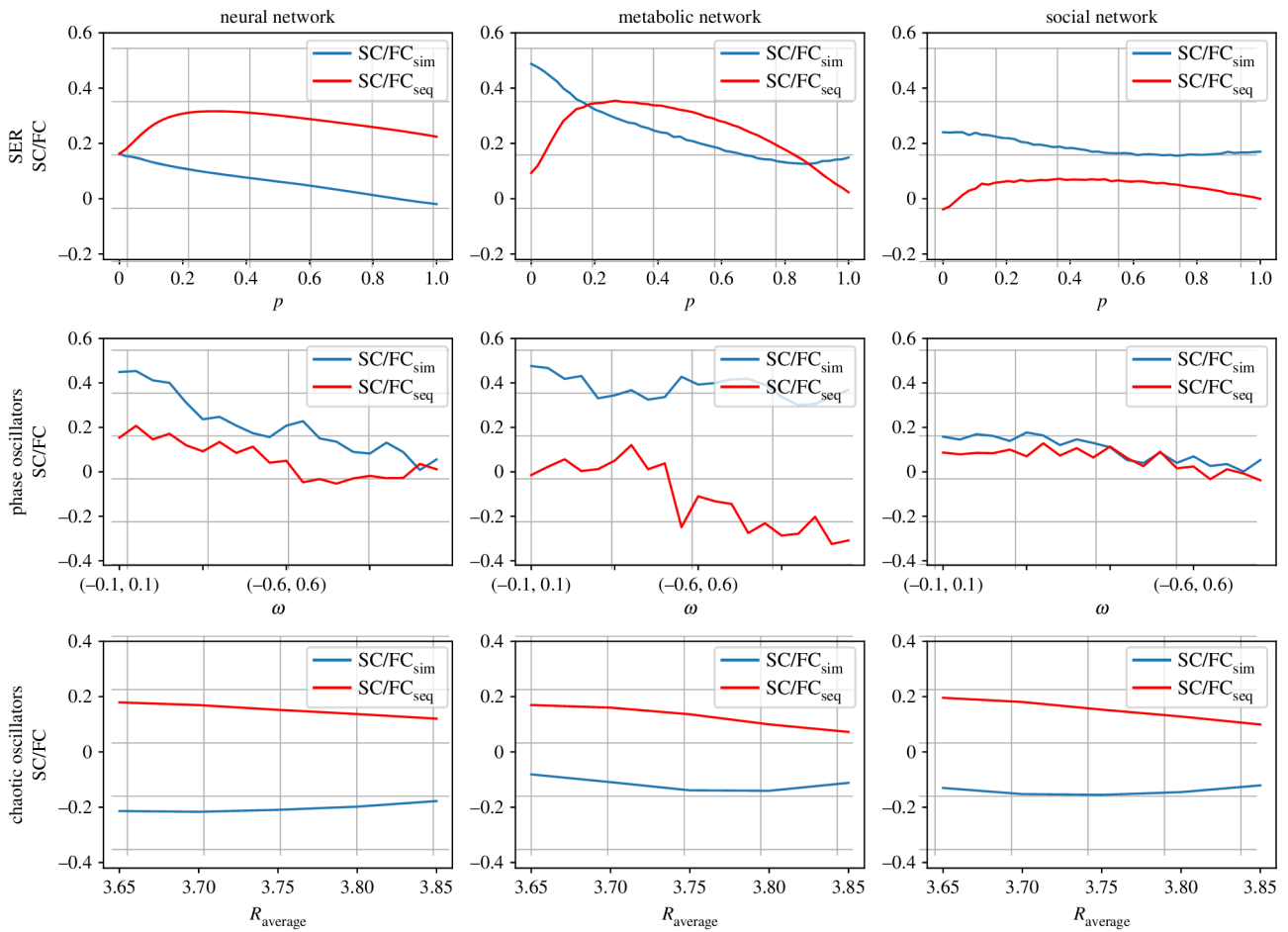
Figure 7. SC/FC$_{sim}$ and SC/FC$_{seq}$ correlations for the three real-life networks under changes of dynamical parameters in the three models, as in §2.3. First column: neural network. Second column: metabolic network. Third column: social network. First row: SER model; parameters: $t_{max} = 10$, N_R (over different initial conditions) = 10 000, $f = 0.001$. Second row: coupled phase oscillators; parameters: $t_{max} = 50$, $N_R = 100$ (over different initial conditions), $k = 10$, $\sigma = 0.25$, $u \in (0, 1)$. Third row: logistic map (chaotic oscillators); parameters: $t_{max} = 500$, $N_R = 50$ (over initial conditions), $k = 2$.

surface and within the near-surface zone. On steeper slopes, these structurally connected pathways are predominantly controlled by the topography and vegetation, whereas on slopes ($ca < 5°$) other surface characteristics such as micro-topography and soil hydraulic properties can become relatively important. The dynamical processes occurring over this structural template and subsequent functional connectivity are then an emergent property of these structural controls in combination with dynamical inputs (e.g. precipitation). The presence of vegetation also (i) modifies soil properties, (ii) often has an associated microtopography and (iii) can impede/reduce flows due to friction and damming effects, so that there are dynamic feedbacks between the structural and functional connectivity [12,13,60].

There are various approaches to assessing structural connectivity in hydrology and geomorphology. If we take a river network, the structural connectivity of the network can be defined based on the pathways connecting all links through which water can potentially flow, resulting in a graph structure most often in the form of a tree [61,62], with the exception of braided streams [63], deltas [64,65] or, for a more broad example, coastal sediment pathways [66]. Thus, the structural connectivity of river networks can be quantified using, for example, the pairwise connectivity of its underlying tree structure—an approach that has been used both for natural and synthetic river networks [67]. These synthetic networks are useful as they inform our

mechanistic understanding of these complex systems. One such example is optimal channel networks (OCNs), which can be generated for varying values of the energy exponent (a parameter that characterizes the mechanics of erosion processes in channel formation) in order to reveal how such topological factors lead to emergent network properties [68]. OCNs replicate the major scaling features associated with river networks around the world [69,70], and thus bridge the gap between random graphs shown in figure 3 that go from structured to unstructured network topologies and river networks observed in nature. Furthermore, river networks have a directional structural template, with links connecting high-elevation nodes to low-elevation nodes. On hillslopes, structural connectivity has been measured based on the upslope contributing area to a particular node (e.g. [71]), and on the combination of topographically connected flow paths (using flow routing algorithms) and the presence of vegetation (measured using remote sensing techniques) that intersects (and in certain environments disconnects) these flow paths (e.g. [72]). Similarly, in hydrological analysis of sub-surface flow, structural connectivity of a network of wells may be determined from the downslope direction of surface topography from any well (e.g. [73]).

In these examples from hydrology and geomorphology, we are concerned with (1) areas that have a similar response to a dynamical probe (e.g. rainfall event) and (2) connectivity of fluxes, i.e. flows of water and/or sediment that are

transported through the network to a downslope/stream location. These two types of functional connectivity map onto FC_{sim} and FC_{seq}, respectively. Approaches used to measure FC in hydrology and geomorphology are varied.

In relation to (1), FC_{sim} geostatistical analysis is often used to assess how the scales of co-activation change in response to a dynamical probe. For example, one can measure the autocorrelation of soil-moisture content and how this changes over time, both in response to a rainfall event and then during a refractory period (see for example [74]). In the case of sub-surface flows, FC between two wells (nodes) a and b is deemed to exist if well b is downslope of well a and the wells are co-activated (i.e. water is present in both) (e.g. [75,76]).

In relation to (2), FC_{seq} is often assessed/inferred based on gauges within a network being activated at a range of lag times, thus indicating the flow of water or sediment between the two locations [77]. Geostatistical analysis has also been used to quantify how FC_{seq} changes throughout a flood event [67]. The FC_{seq} of fluxes through a real or synthetic river network has also been simulated and incorporated into a dynamic tree approach by analysing dye propagation models at successive snapshots [78]. Such approaches could be particularly valuable for studying the little understood impact of pulses of sediment [79], nutrients [80] or other diffuse chemicals [81] transported by surface waters. In the case of sub-surface flows, sequential activity of the two wells may be inferred from time-series analysis of water levels at a range of time lags (e.g. [73]).

Suitable empirical data for measuring these examples of functional connectivity are relatively scarce, and therefore researchers often turn to process-based modelling as a way to quantify both types of functional connectivity. For example, high spatio-temporal resolution modelling can be used to measure times during a storm event when infiltration will be locally satisfied and thus the onset of runoff generation (excited) or not (susceptible/refractory) due to spatial variability in infiltration capacity, rainfall intensity and antecedent soil-moisture content. From this high spatio-temporal modelling, the degree of synchronized functional connectivity of all locations within the model spatial domain can be derived. The spatial pattern of these synchronized points in turn determines the sequential connectivity of runoff and sediment flux [82,83]. For example, using high-resolution process-based modelling [21] measured the length of connected flow paths on grass and shrub hillslopes that had varying lengths of structurally connected pathways. In this example, the longer the SC, the higher the FC_{seq} of discharge and sediment flux, which is similar to that observed in the case of coupled phase oscillators where FC_{seq} is destroyed with an increase in the randomness of the network.

Whereas some evidence exists for the impact of SC on FC_{seq} at a particular timescale [21], there remains scope to examine patterns of FC_{seq} both at increasing lag times and in response to dynamical probes of different magnitudes for their impact on landscape change (topological changes). Furthermore, geomorphological assessment of the importance of coupling strength among nodes remains unexplored. An important point to highlight is that timescales of synchronized versus sequential functional connectivity in hydrology and geomorphology are often markedly different. The widespread synchronization of activity over a spatial range is valid for a small time period (mins/hours), while the sequential

propagation of fluxes through the network occurs over longer time periods—hours to days to decades—depending on the size/configuration/connectivity of the network/ system. Similarly, earthquake/storm-driven landslides tend to be synchronized over timescales of hours–days, whereas the resulting cascade of material through the network is sequential over significantly longer timescales (e.g.[84–86]).

Likewise, the spatial scales associated with synchronized and sequential connectivity tend to differ. For example, nearby nodes often exhibit synchronization, whereas sequential flux propagation is observed at a larger spatial scale [87]. Flood events highlight the potential for sequential propagation of processes over large spatial scales over time periods of hours to days. In catastrophic flooding in the Lockyer valley in Queensland, Australia in 2011, the hydrological and sedimentological connectivity between the channel and the floodplain was spatially variable depending on the morphology of the reach and whether it was expanding or contracting [88]. Hence, in this example, the organization of dynamical processes in the network was crucial to the change in channel morphology, despite assumptions that in such a large flooding event thresholds for connectivity would have been exceeded.

3.2. Application to freshwater ecology

Over the decades, ecosystem ecology has developed a considerable amount of methodologies for network analysis, which contributed to the characterization of the evolution and status of ecosystems [89]. The structural connectivity (SC) is represented in these models by depicting standing stocks (e.g. biomass, local communities or populations, species, individuals, or habitat patches) as nodes, and the interactions between them (e.g.feeding, the movement of animals or diseases) as links [89]. Within landscape connectivity, the spatial structure of river networks (SC) plays a key role in structuring ecological patterns [90]. Graph representations of river networks are often modelled to resemble the hierarchical structuring of habitat patches (nodes) and the potential dispersal corridors (links) [91–95].

Dynamical approaches have not explicitly used the terms co-activation or sequential activation for describing functional connectivity. However, some of the notions in this paper can also be deduced from dynamical approaches of habitat connectivity already applied in aquatic ecology. The focus on animal movement and dispersal has been driving the theoretical and empirical work in the past few decades [62,93,96–100], especially in the light of fragmented landscapes. In models of organismal–environment interactions based on landscape's resistance to dispersal [101,102] and in models that include the intrinsic dispersal abilities and limitations of organisms (i.e. individual-based population or metacommunity models [90,103,104]), the movement of animals is represented as the dispersal of individuals from node to node (analogous to the flow of vehicles in a transport network [97]).

Community ecologists have long seen individual populations and communities as oscillators [105]. They focused on the dynamics of a modular network, inferred from the synchrony between the rate of change of the population density within nodes [105]. Another example is the ecohydrological study of [103], where they proposed the concept of 'fluvial synchrograms' to explain patterns of the geography

of metapopulations' synchrony within a river network, using the case of freshwater fishes of Europe. In their empirically driven approach based on the geography of synchrony, they developed theoretical synchrograms using simulated time-series of species abundance from the spatially explicit dynamic metacommunity model [103]. These fluvial synchrograms depicted the decay in synchrony over Euclidean, watercourse, and flow-connected distances [103]. Synchrony was higher in populations connected by direct water flow and decreased faster with the Euclidean and watercourse distances, highlighting the extent of spatial patterns of synchrony that emerge from dispersal [103]. Other approaches like the ones of [103,105–108] are examples of investigations focused on the effect of the network topology (SC) on the synchronous dynamics of nodes (FC) (SC/FC relationships). Representations of synchronous functional connectivity go beyond the movement-based approaches and can include models using the input–output analysis described in the ecological network analysis (ENA) section (§3.5.2) (i.e. species interactions models quantifying predator–prey, mutualistic or competitive relations [109]; species–resource interactions models quantifying consumer–resources relations [110–112]; food webs models that trace energy movement [113–115]; and nutrient cycling models [116]). In competitive consumer–resource systems, consumers can overlap their diet and resources interact with one another, which makes it possible to visualize them as coupled oscillators [110,117]. To explain the dynamics of communities in these systems, Hajian-Forooshani & Vandermeer [110] applied the enduring Lotka and Volterra equations [111,112] and the Kuramoto model [118] in a simplified three-oscillator system. In this system composed of three consumers and three resources, they measured two distinct types of coupling: trophic-coupling (the strength of cross-feeding) and resources-coupling (strength of competition between resources) [110]. Given a persistent oscillator in the Lotka–Volterra formulations, trophic-coupling implied eventual synchrony (all oscillators are in the same point in circle space) and resource-coupling implied asynchrony [110]. The simulations in both of the two models had similar results, suggesting that coupled oscillators and the application of the notions of the Kuramoto model can provide theoretical contributions on ecosystem and community organization [110].

To illustrate the idea of sequential activation in freshwater systems, we consider examples using random walks. Random walk is the most common approach to simulate animals' movement and can be considered as sequential FC, since the sequential steps of their dispersal can provide valuable information about the network structure. For theoretical studies that model the distribution of local species' persistence in time, random walk without drift is the simplest baseline demographic model [119]. In originations and extinctions models working with macroevolutionary timescales, the abundance of a species in a node has the same probability of increasing or decreasing by one individual in each time step [119]. Then, the increase of one individual will represent the colonization of a free site by an individual of a new species in the system, or a randomly sampled individual within the community [119]. An assumption of this model to account for limited dispersal effects is that only offspring of the nearest neighbours of the dying individual are allowed to colonize the empty space [119]. Additionally, the local extinction corresponds to a first passage of a random walker equal to zero, leaving a persistence time distribution

following a power-law decay with exponent 3/2 [119]. A simpler alternative model will be the stochastic patch occupancy model (SPOM) that describes the presence/absence of a focal species in a node (simulates only colonization and not colonization–extinction dynamics) [120,121]. Here, in a given structural river network with discrete habitat patches as nodes, each node has a probability to be colonized by species belonging to the regional species pool [120]. At the starting point of each simulation, a sequential colonization process starts. From initially occupied nodes, or initially introduction sites of the new species, the empty patches can become occupied in a sequential manner (successive snapshots). The potential occupancy of a node will be dependent on a chain of colonization events and the presence of unoccupied nodes within a certain range (only empty nodes could become colonized). The SC/FC relationships implied by the aforementioned studies are different from the ones described in this paper. The dispersal of animals (which serves as sequential FC) finally determines the structure of the network and in the approaches of [115] and [114] this one is built using time-ordered graphs (i.e. continuous-time Markov chain for [115]). The main difference is that this provides a time-resolved view of the dynamics, whereas in the approach of the current paper, the time is eliminated by suggesting the time-average view on dynamics. Bridging over these two types of time views on dynamics requires further investigation on how the FC that derived from the temporal graphs contributes to the time average information of dynamics. Ecological applications of dynamical approaches, like the ones mentioned above, and the classification of the two types of FC addressed in this paper bring new perspectives to assess functional connectivity in freshwater ecology. Additionally, evaluating the SC/FC relationships can highlight the importance of specific nodes in facilitating the overall colonization processes, which can help to estimate a number of effective reserves necessary to achieve a particular conservation goal [103,122–126].

3.3. Application to systems biology

In systems biology, we find many instances where a distinction between simultaneous and sequential events in networks is made, even though the terminology of 'functional connectivity' is rarely used. On the level of *gene regulation*, for example, temporal programmes structurally implemented via single input modules [127], leading to a 'just-in-time' production of proteins for specific biological functions in a bacterial cell [128] are an example of a contribution to functional connectivity based on sequential activation. Note that here the unweighted graph would lead to a misleading relationship between structural and functional connectivity, as structure in the *unweighted* graph would suggest a co-activation, rather than a sequential activation. The latter, in fact, is implemented via distinct weights from the regulator to the target genes or operons. As we see in all the case studies presented here, such details matter, when bringing these abstract concepts to a specific domain of application.

Another example is the sequence of events during the yeast cell cycle, which is hard-wired into the corresponding gene regulatory network [129] and can be understood using simple, discrete cellular automata-type models [130,131], namely Boolean network models [132].

A more common approach in systems biology addressing the relationship of gene expression (or transcriptome) data—simultaneous measurements of gene activity via high-throughput technologies—and the underlying regulatory network is network inference. This approach summarizes a range of statistical methods to infer the regulatory network from expression profiles [3,133]. It should be noted that this approach already starts with assumptions about SC/FC relationships, in particular, that indeed structural connectivity can be reconstructed from observations of the dynamical states [134].

In the case of *metabolic networks*—bipartite graphs of metabolites and biochemical reactions available in a cell, where reactions can be represented either by enzymes or by the genes encoding these enzymes [33,135,136]—the activity levels of genes encoding enzymes can be thought of as a representation of the metabolic state of a cell. These activity levels are given by transcriptome data. Statistical analysis of transcriptome data (either by repeated measurements—replicates—or by contrasting the cellular condition with a baseline or reference conditions (e.g. mutant gene expression levels with wild-type gene expression levels)) leads to sets of genes characterizing a cellular state, for example, the sets of 'upregulated' and 'downregulated' genes or the sets of genes with 'high' or 'low' expression levels within a large set of samples. A possible definition of functional connectivity then is the induced subgraph of a gene-centric projection of the metabolic network spanned by such a gene set derived from transcriptome data [137].

The connectivity of such a subgraph compared to randomly drawn gene sets is a convenient and frequently employed measure for SC/FC correlations in this context [7,138–140], as it addresses the statistical question of how clustered such a gene set (representing functional connectivity) is within a given (metabolic) network (representing structural connectivity).

The conceptual model of functional connectivity behind such an investigation is that of synchronous activity. Distinguishing between the two types of functional connectivity is challenging, given the current state of 'omics' data in systems biology, due to the lack of suitable time-resolved data.

This observation is further underlined by the fact that predictive theories of genome-scale metabolic activity (e.g. flux-balance analysis, [141,142]) are also based on a steady-state assumption. In order to discriminate between co-activity and sequential activity, one needs to resort to time-resolved models, typically based on ordinary differential equations (ODEs), which, however, due to their often huge number of required parameters are restricted to single pathways or other suitably defined cellular subsystems, rather than the scale of a whole cell.

Beyond these two basic situations characterized by a gene regulatory network and a metabolic network as structural connectivity, respectively, there are many other examples of sequential and synchronous usages of a given 'hardware' in systems biology. Metabolic control analysis [143,144] relates the distribution of control in biochemical networks to their structure. Protein interaction networks [145] summarize how selective binding patterns (structural) and protein complexes (the dynamic assemblies to execute biological function) are interlinked. Fermentation processes (e.g. in cocoa fermentation) often rely on a sequential activation of microbial populations [146].

Summarizing the SC/FC situation in systems biology in a qualitative form, one can conclude that gene regulatory networks lean towards sequential activation, while protein interaction networks functionally lean towards co-activation (protein complexes) and metabolic networks may display aspects of both (steady-state activity versus metabolic pathways).

3.4. Application to Neuroscience

Neuroscience is one of the first disciplinary fields in which the need to formalize notions of SC and FC was felt. Perhaps this was due to the fact that network descriptions in neuroscience go beyond a mathematical representation but correspond to an actual, concrete reality: neural circuits are networked systems, with their 'reticular' (from Latin for 'little net') nature debated since at least the turn of past century [147]. Network nodes can be, depending on the scale of observation, individual neuronal cells (at the micro-scale), populations involving thousands of neurons (at the meso-scale), up to entire brain regions (at the macro-scale). The relations defining links are different depending on the considered type of connectivity and are defined both in terms of anatomy of wiring and of information exchange.

It is natural to consider SC in Neuroscience as the description of anatomical connections physically existing between network nodes: individual synaptic connections forming electrochemical junctions between the outward axons and the inward dendrites of different neurons (within volumes $<$ 1 mm^3, already containing approx. $10^4 - 10^5$ neurons); or bundles of long-range connection axons coupling together smaller or larger groups of neurons, separated by varying distances (approx. $1 - 10$ mm for mesoscale circuits up to approx. $10 - 100$ mm for macroscale, brain-wide networks). At all these scales, one usually refers to the compilation of all structural connections between probed network nodes as to a connectome [148,149]. Different techniques must be used to extract SC information at different scales, even if a systematic review of them is not possible here. We can briefly mention, though, that we dispose of whole matrices of SC for rodent, nonhuman and human primate brains [32,146–151], as well as detailed microcircuit reconstructions [152–154].

Studies of SC in Neuroscience often revolve around: the search for general architectural [159] or wiring optimization [160,161] principles in connectivity, or the identification of characteristic motifs of connectivity that are over-represented with respect to chance-level [162,163] and special structures such as dense clusters at the micro-scale level [164], or cores and 'rich-clubs' at the macro-scale level [151,165]. Recently, attempts have also been made to use topological data analyses techniques [166,167] to characterize the 'shape' of networks beyond the limitations of graph theoretical descriptions, which greatly emphasize strictly local or strictly global aspects but are deficient in capturing intermediate structures at arbitrary meso-scales. Other lines of research aim at linking specific structural motifs to specific functions, as in the case of specific arrangements of positively weighed excitatory connections and negatively weighed inhibitory connections allowing modulations of perception [168] or of specific patterns of interconnection between cortical layers at different depths in the tissue thickness, allowing the regulation of sensory and predictive information flows [169]. Finally, many efforts have been devoted to identify SC alterations that may be indicative of developing and progressing

neurological or psychiatric pathologies, and thus serve as diagnostic or predictive biomarkers [165,170]. However, a comprehensive survey of all these applications largely transcends the scope of this review.

Not only are neural network nodes (neurons or populations) wired together by living cables, but messages are continually exchanged along these cables. All information processing related to our perception, our cognition and our behaviour is generally believed to arise from the exchange of 'spikes'—propagating pulses of electric depolarization of the cell membrane, able to elicit neurotransmitter release at synaptic terminals—between synaptically connected neurons. Such spikes, individually or grouped in more complex spatio-temporal patterns, represent 'codewords' encoding information about external and internal worlds in still largely unknown languages. Streams of spike-encoded information are thus copied, transferred and merged between system's components linked by SC, assembling into emergent neural algorithms that ultimately underlie functions and behaviours [171]. These computations are highly distributed and the communication between system's units that they involve can also be seen as giving rise to networks, but this time of functional rather than structural nature. Two units are thus defined as functionally connected if they 'interact'. The problem is therefore to operationally define how an 'interaction' can be pragmatically measured from observing how coordinated neural activity unrolls through time.

Some measures of FC define 'interaction' as 'synchrony' between activity fluctuations and modulations. This is the case for instances of so-called resting state FC [172], describing linear covariance between the fluctuations of different brain regions during unconstrained mind-wandering, as revealed by functional MRI (fMRI). Such metrics of connectivity are akin to the first form of FC previously described. Given the remarkable oscillatory components present in an neural activity and simultaneously at different frequency bands [173,174], analyses of synchronization-type FC in neuroscience are often conducted in the spectral domain, tracking coherence and phase-locking [175]. Individual neurons are not necessarily oscillating and can keep firing in irregular manner, nevertheless neuronal populations can collectively oscillate because of the interplay between excitatory and inhibitory currents within local recurrent microcircuits [176]. Such collective oscillations produce periodic modulations of the excitability of neurons within large populations, so that efficient transmission between synaptically coupled populations can occur only if their respective local oscillations are suitably aligned in phase ('communication-through-coherence' hypothesis [177]). Thus, two neuronal populations that are structurally connected may become functionally disconnected if their oscillations are, for example, in antiphase and spikes emitted in proximity of the sender population's oscillation peaks reach postsynaptic neurons at the throughs of the target population's oscillations and hit thus against a wall of locally generated inhibitory blockade, preventing information carried by input spikes from being transduced into output activity. Under this hypothesis, it is thus possible to flexibly 'switch on and off' FC on top of a static SC link, just by adjusting the relative phase of the sender's and target's oscillations. A natural generalization of linear correlation from the time to the spectral domain when dealing with oscillatory neural activity is inter-regional coherence or phase synchronization

[175]. Coherence in the gamma band (40–100 Hz) between frontal/prefrontal and sensory regions is known, for instance, to be boosted in sensorimotor coordination or attention [178,179]. Furthermore, FC can also be established between populations oscillating at different frequencies via nonlinear cross-frequency coupling [180]. Not only cognition but also pathology can perturb coordinated neural oscillations and the associated FC [181], but once again a detailed coverage of the use of oscillation analyses for biomarking goes beyond the limits of the present work.

Other measures of FC go beyond mere synchrony or correlation—beyond the first form of FC—and attempt reflecting actual causal influence. Unlike correlation, which is symmetric and thus gives rise to undirected graphs of FC, measures of causal interdependence between time series of neural activity give rise to directed networks. In Neuroscience, 'functional' and 'effective connectivity' are sometimes used as distinct terms, with the latter serving as a FC measure that tracks causality. However, here, we keep naming connectivity of functional type all connectivity relations that do not express anatomical interconnection. A very simple way to account for the direction of interaction can be to assess the temporal precedence of the 'causing' on the 'caused' fluctuation. This can be achieved for instance by using lagged cross-correlation or mutual information rather than zero-lag correlation (e.g. [183]), since the effect cannot precede the cause. In this sense, these metrics are related to the second form of FC, reflecting sequential activation, as previously discussed. However, the correspondence is only partial, in this case and unlike for neural FCs of the first form. If exact sequences of neural activation can be produced by neural architectures known as 'synfire chains' [184], they have been only rarely sought for in actual recording and neuroimaging data [185,186] and not been put in relation with notions of functional coupling. Directed FC measures in neuroscience are defined operationally in terms of time-series-based statistical metrics, rather than in terms of explicitly dynamic considerations. Thus, while in many cases the statistically-inferred directed FC goes, for example, from the phase-leading to the phase-lagging neuronal population [187,188], i.e. respects a sequentiality criterion, in other cases the relation can be inverted, reflecting nonlinear interactions between populations, as anticipatory synchronization [189] or heterogeneities in internal synchrony levels [190]. More explicitly, causality could be captured: by the detection of remote effects on distant regions triggered by interventions in local regions (as in dynamic causal modelling [182]); or by showing that consideration of the past activity of a putative causal source region improves the prediction of the future activity of a target region, as in Granger causality analyses of neural time series [191–193]. Importantly, Granger causality can also be spectrally decomposed [194], allowing the detection of the contribution of different oscillatory components of neural activity to inter-regional causal influences. It has thus become possible to observe that causal influences in different directions can be mediated by oscillations in different frequency bands, e.g. in the gamma-band (approx. 40 Hz) for bottom–up and in the beta-band (approx. 20 Hz) for top–down information exchange between prefrontal and visual regions [195,196].

More recently, emphasis has been put on the fact that FC networks are not static but change in very flexible ways through time, i.e. they are better described as temporal networks [197].

The new term of 'chronnectome' has been introduced to stress how, beyond analyses of the static functional connectome, explicit consideration of the spontaneous reconfiguration dynamics of FC over time may help to better discriminate cohorts of subjects and patients, by disentangling temporal from inter-subject variability [198]. At the macro-scale, different FC networks are sequentially recruited along the unfolding of cognitive tasks, potentially signaling different neurocomputational steps [199,200]. Spontaneous resting state FC networks wax and wane in a seemingly stochastic flow that is not randomly structured but displays characteristic long-term memory [59] and whose rate of reconfiguration and degree of temporal structuring predict cognitive performance at the single subject level [201,202]. At the micro-scale as well, the emergence and dissolution of transient synchronous assemblies of cells within hippocampus and enthorinal cortex can be modelled with temporal network descriptions [203]. Future studies will be needed to understand whether this complex FC network dynamics can be seen as a measurable fingerprint of ongoing neural computations linked to functional behaviour [204].

The definitions of SC and FC given in the previous subsections are in principle completely independent: one could indeed assess the existence of FC based on the analyses of multivariate neuronal activity time series without knowing anything about the underlying anatomy and SC. This scenario of a 'perfect separation' between SC and FC is obviously unlikely. However, an equally naive scenario dominates the discussion of many articles in the literature in which a structural cause is necessarily sought for to explain any change arising at the level of FC. In reality, the flexibility of FC on very fast behavioural time-scales with respect to physiological processes reshaping SC (at least at the meso- and macro-scales) already suggests that FC cannot just be a passive mirror of the underlying SC. We have previously proposed that FC is the measurable by-product of underlying collective dynamics [187,205]. In this proposed theoretical view [206], alternative modes of a system's dynamics, or states within the 'dynome' [207]—or dynamical repertoire [208]—of a system would give rise to alternative FC configurations on top of a same underlying SC (functional multiplicity).

Analogously, circuits with very different SC but that give rise nevertheless to equivalent dynamical modes—a property known in systems neuroscience as functional homeostasis [209]—would give rise to similar FC (structural degeneracy) [210]. An example of degeneracy can be found in simulations of neuronal cultures *in vitro*, in which high clustering of FC is invariantly found because of collective network activity bursting, independently from the simulated culture's SC being weakly or strongly clustered [211].

It is important to stress that, in our view, FC goes beyond the level of the node-specific dynamics and includes collective dynamical modes of the entire neural system. This is made evident in studies that attempt to predict large-scale FC in spontaneous resting-state activity conditions starting from simulations of SC-connectome-based simulations. In these cases, a good fit between simulated and empirical FC is obtained only when the model is tuned to operate close to a critical point of dynamic operation [212,213], indicating that FC manifests a peculiar dynamical regime, certainly shaped but not fully constrained by structure. For instance, waves [19,20] or 'connectome harmonics' [214] shape large-scale coordinated activity and, hence, FC. The importance of being tuned into specific dynamical regimes to account

for the qualitative features of large-scale coordinated activity has also been confirmed by minimal models, with reduced realism but enhanced possibility to rigorously understand mechanisms [27,28,215]. A predicted consequence of this hypothesis is that local perturbation to individual nodes within a neural network may induce a network-wide reconfiguration of FC, including of remote nodes not directly connected to the perturbed node [205]. In a nonlinear system the exact same perturbation can lead to different effects in different dynamical states and since the FC clearly depends on the dynamical state of the system, the effects of a local perturbation can be dependent on FC rather than on SC. Once again, computational simulations of virtual brain models informed by empirical SC information but augmented with nonlinear brain dynamics confirm the validity of our prediction [216]. Virtual brain models tuned to regimes maximizing the degeneracy of their 'dynome', sampled via a noise-driven exploration, also succeed in qualitatively reproducing the switching 'chronnectome' observed in resting state fMRI [217]. Computational modelling thus provides strong evidence in favour of our hypothesis of flexible FC being the by-product of a complex dynamical system, whose behaviour is constrained but not fully determined by the underlying SC. In other words, function follows dynamics, not structure.

3.5. Application to social-ecological systems

Social-ecological systems (SES) are complex adaptive and multilevel (polycentric) systems attributed with interplays between human and non-human entities (nodes) at spatial and temporal scales [218], through the metabolic flows of material and energy (links). The concept of 'social metabolism', taken from cellular metabolism, is central in the study of SES [219]. Network analysis has increasingly been used to study coupled, or social-ecological systems [220–224]. Here, the SES is often depicted as a multilevel social-ecological network (SEN), where social/human actors comprise one network, natural entities a separate network, and flows are captured between and within each network level. Such multilevel networks are modelled via a stochastic environment, such as a Multilevel ERGM [225]. Here, micro-configurations are specified, consisting of actors and/or entities from either or both the two networks, such as the tendency for two social nodes to share a coordination tie when both nodes are likewise linked to the same natural resource. These microconfigurations are then modelled, alongside other competing tendencies (such as the general tendency of a network to exhibit transitive closure), to test hypotheses linking SEN patterns to sustainable (or unsustainable) management practices.

3.5.1. Social networks

The standard SC/FC approaches are usually uncommon in social networks because the distinction between the 'hardware' (structural connectivity) and the dynamics (functional connectivity) is less clear than in other fields. However, measuring the (often rapid) flows along the edges of a more stable (slowly changing) network, as the example of the competence perceptions and the everyday information exchanges in a company shows, could be an interesting perspective for future research approaches, incorporating two theoretical frameworks: social systems theory [226,227] and SNA [54,228,229], e.g. in the context of relational events models [230].

Both approaches are debating how the internal function (of networks or systems) can produce emergent properties that transform the structure and vice versa. However, in social science, these debates are not without tensions (i.e. between structure and agency) and criticisms (i.e. by more conflict-oriented approaches). We argue that the overlap between 'system' and 'network' could be helpful for SC/FC in social science, specifically to understand the connections between actors embedded in different social subsystems and how underlying network topologies among those actors impact the subsystems (for example, economy and democracy), and *vice versa*. Signed contracts between public institutions (PI) and private companies (PC) can serve as an illustrative example. The outcome of a relational analysis of public procurement is a multilevel, multi-relational, two-mode network of business–government connections, whose nodes and relations are embedded in different social subsystems: the economic system, the political system and the State. Here, the main focus is the SC/FC relationships that emerge from the analysis of the procurement network.

FC_{seq} is the longitudinal and dynamic procurement process, analysing the sequential configurations to understand why a PI is issuing a contract, whether to one and not to another PC. Some of these companies could be important market leaders or potential corrupters. FC_{seq} is especially significant in the case of private actors, as we assume that very outstanding degree-peaks of a few companies could be evidence of a corrupted network dynamic. Companies with an extraordinarily high number of contracts in a short period may have extraordinary political influences (i.e. interlocks or bribes). Both the relational positions and the dynamical peaks could correlate directly to structural network transitions (collapse or even fragmentation) and also to system-related implications, such as the resource distribution in the economic system or the decision-making process in the State. FC_{sim} is the specific linkage-configuration at each time step: nodes that have active links to the same node(s) are co-active. The co-activation through shared links is changing in each time step when a new link is created, and an existing link is decaying. FC_{sim} applies to PI and also to PC, and can be seen as an indicator for strong relational positions of other nodes (in the opposing type) in the network. For example, many co-active institutions are a 'pointer' to influential companies, whether important market leaders or potential corrupters.

3.5.2. Ecological networks

Ecological network analysis (ENA) is a systems-oriented methodology developed by ecologists to understand whole-system dynamics and properties [231,232]. This methodology is based on network and information theory and derives itself from input–output analysis, modelling ecosystems as a set of nodes and ties (vertices, edges) [233,234]. Under this framework, species, aggregation of species into functional groups, or non-living resource pools are taken as nodes while the exchange of material or energy between species is taken as edges. In addition, ENA methodology has also been widely applied to analyse direct and indirect exchange of energy and carbon emissions between economic sectors at urban/country level from a system perspective [235]. This methodology is useful to evaluate system properties such as cycling index, total throughflow and relational interactions by pair-

wise components in the system through thermodynamically conserved transactions of a chosen currency [236].

Although not explicitly using the language of structural connectivity and functional connectivity, ENA internal logics resemble those used in connectivity science [21]. Under the ENA framework, SC is defined by the number and position of functional groups—species, aggregation of species or economic sectors—forming the nodes and the flows of material and energy between them (edges) [231]. This set of arrangements defines the network architecture or network topography and, therefore, the 'hardware' on which dynamic processes take place, normally represented with an adjacency matrix [114,231]. Ecosystems are open, thermodynamic, far-from equilibrium systems, which implies that they require continual input flow of high-quality, low-entropy energy [237]. Once energy enters the system, it is the structural connectivity that defines the system's overall dynamic flow-storage patterns [236]. ENA is applied to steady-state systems, therefore capturing, in a snapshot, both the structural connectivity and the cumulative behaviour of a given highly dynamic network.

Now, we turn to the functional connectivity under the ENA framework, employing a basic input-state-output model frame. As open systems require continual input, an ecosystem is sustained by the dynamic co-activation pulses entering across the boundary. In nature, these pulses could be seen as the solar energy received by the primary producers (multiple individuals or multiple species, depending on scale). In this manner, we interpret co-activation as nodes sharing a functional similarity, such as trophic level, and thus being charged simultaneously. This is different from viewing co-activation as two or more attributes to align for activation to occur. The latter may not have a direct analogy in ENA. In this case, the input of energy is simultaneous to several nodes due to their inner characteristics (e.g. they all belong to the same trophic level). Once co-activation occurs, the energy/material flows sequentially from node to node. Although ecological networks have complex connection patterns including cycling, each individual sequential pathway can be 'decomposed' and identified as a unique carrier of energy matter from initial activation to final dissipation beyond the system border. These energy flows are the base of all exchanges and form the model structure encompassing a diversity of nodes and trophic levels. The sequential activation is captured along these cascading indirect pathways from the initial co-activation pulse. Therefore, the most straightforward way to visualize functional connectivity based on the sequential activation of nodes is with a linear food chain. The initial input of energy triggers the sequential activation of nodes down the food chain, whereas each component is dependent on the previous for its flow source [237]. Eventually, as the initial pulse travels throughout the many networked pathways, it is dissipated, its useful energy spent, coming to rest outside the system boundary (as higher entropy) and completing the input-state-output triumvirate. Ecological network analysis can expose some of the interesting properties that emerge in the state based on those input–output relations.

What is particular about ecological, and therefore also SES, systems and networks is that one major element conditions both their architecture and their functional connectivity over the long run: net energy (as an indicator of low entropy) [238–241]. As long as there are high levels of net energy, connectivity (and therefore complexity in terms of nodes and

functions) can increase, as new 'agents' or 'elements' are attracted to the system or drawn into it by existing agents.

Nodes that happen to (or managed to) control large amounts of net-energy flows can leverage their relative position in the network and exert power over other network members. This means that such agents then have substantial power to adapt the network architecture to their own preferences, e.g. to increase their relative power [242]. It acts collectively on major sets of nodes, thus it contributes to synchronous FC, but it can also trigger cascading effects within the network, contributing this way to sequential FC. Power enables agents to exert a certain level of control over other agents and even allows them to eliminate or add other agents or nodes. In particular, they may control the distribution of flows as they move through the system.

3.5.3. Social-ecological networks

A rich body of literature on social-ecological system analysis focuses on the structures and patterns of interdependent social and ecological interactions (SC), which are further associated with phenomena of interests like cooperation and conflict [223,243–246]. More specifically, it investigates the actor-to-actor relationship in the social system, the ecological component-to-component interdependencies in the ecological system, as well as the actor-to-component relationship across the social and ecological system [247]. Altogether it forms a multilevel network configuration made of nodes and links between different system entities. In terms of SC/FC relationships, one line of research is exploring how certain social–ecological system configurations can facilitate successful adaptation and transformation in SES to address resource management challenges [243,248,249]. Both adaptivity and transformability are critical elements of resilience study, describing the capacity of the interdependent social–ecological systems dealing with unknown or unforeseen shocks [250,251].

Although using different terms, other lines of research have identified two types of cascading effects that connect various regime shifts, the directional and bidirectional links [252,253]. One is called the domino effect, which reveals a one-way directional dependence [254]. We argue that it fits more with sequential functional connectivity because the feedback from one regime shift affects the drivers and outcomes of another regime shift, while the other one is termed hidden feedback, showing a self-amplifying/damping bidirectional cycle [246,255], which we argue is more of a synchronous connectivity nature.

Various analytical frameworks have been applied to capture the process of co-evolution, such as the MuSIASEM (multi-scale-integrated assessment of societal and ecosystems metabolism) framework. From a MuSIASEM perspective, flows of material and energy move through a system (or network) in order to fulfil certain societal functions. We argue that it departs from a set of known structural connections (e.g. the mix of primary energy sources for a society and its end uses) and then tries to describe functional connectivity of a central element of a network structure by using ratios that are composed of both a flow and a fund element. Flow is the element that either disappears over the duration, such as primary energy, or appears by the end of the duration like the product, while fund can be seen as a converter that transforms input flows into output flows during the enter–

exit duration, e.g. labour, land or machinery. Moreover, funds are impermanent structures whose existence depends on the availability of flows [239]. These ratios give (among other things) information about the relative power of nodes/agents in multi-level networks. High rates of metabolized energy provide increased power to (1) control and both create and synchronously co-activate many nodes/agents in a network (hierarchy–dependency effect) and (2) influence sequential activation by controlling flows (controlling-the-tap-effect). MuSIASEM tries to provide measures and indicators for such relations, in order to guide the transformation towards a Post-Carbon society.

Another concrete example of an SES here is the global commodity trade system connecting resource extraction and final demands. Here, nodes are the trading partners such as cities/countries/regions (at various jurisdiction levels), which can be linked through flows of products, material, monetary value and environmental footprints. Altogether, the established static trading structure with complex interactions constitutes the network architecture (SC). For instance, in the palm oil trading market, Indonesia and Malaysia have been the main producers, exporting products to countries like the EU, China and India. The identified relational structure between the countries is the SC. On the other hand, network dynamics (FC) describe the dynamics of the flow (i.e. the quantity of trade; the environmental footprint) embedded in the relational patterns. Input–output analysis [234,256] has been widely used to capture the input flows among each sector of trade partners in the network. The flow dynamic in the IO table is rather synchronous, in the sense that it is the market interaction where price co-activates both supply and demand sides. For instance, with the EU passing a stricter sustainability regulation while importing palm oil, big producers like Indonesia tend to export more of their products to less regulated markets like China. The network structure remains the same, yet the flow dynamic changes synchronously as driven by the market price (i.e. higher standards will increase the production costs, thus the price will rise accordingly). Sequential activation cannot be modelled using input–output analysis (IOA), as it is more like a snapshot of an economic system in a given moment in time. In fact, this static nature of IOA is often criticized as one of its major shortcomings that have only partially been overcome by the development of dynamic models.

Although connectivity terminology is not explicitly used here, the phenomenon of network evolution through actions of its agents (nodes) is found quite evident. The theoretical framework developed in the paper regarding the distinction between synchronous and sequential events has a great potential to provide a different network perspective to understand the underlying mechanisms in social–ecological networks.

4. Conclusion

Here, we have attempted to unify the broad range of SC/FC approaches within a common framework. We have reproduced key findings from the literature and extended them towards additional variations of network topology and dynamical characteristics in order to see common properties and underlying principles and offer a deep mechanistic understanding of the major contributors to SC/FC correlation.

Minimal models (small toy model representations of certain classes of dynamics) are helpful to explore these generic features. Our challenge here was to describe how the strengths of the two types of SC/FC correlations—based on co-activation and sequential activation—depend on the class of dynamics, the network architecture, the coupling and the internal dynamical parameters. We used numerical simulations to derive some universal behaviours of SC/FC correlations under changes of these system properties and to apply this knowledge to real-life systems or data.

The strength of SC/FC correlations can be shifted between the two classes—functional connectivity based on co-activation and sequential activation—in basically three ways: (1) modification of network architecture (e.g. the gradual randomization of a modular graph), (2) change in parameters of the dynamics (e.g. increasing or decreasing the noise or the coupling) and (3) a change in the temporal resolution in which dynamical data are observed (e.g. by temporally coarse-graining the observed time series).

The basic challenge of this type of investigation is that the strength of each type of SC/FC correlation depends not only on the class of dynamics, the network architecture, the coupling strength and the dynamical parameters, but also on the type of statistics that are applied. In some cases, the effect of the different statistics is so strong that there is a noticeable change in the properties that are preserved or not.

An important question is how to assess the reliability of the results. In order to confirm that a numerically observed behaviour of SC/FC correlations (under systemic changes) is reliable, we performed the following tests: (1) We vary the other system parameters slightly, in order to study the robustness of the result. (2) We reproduce the behaviour observed in a minimal model also in a richer representation of the same class of dynamics.

Of course, the question is more involved on the technical level than our brief introduction hints at. There are different ways of assessing functional connectivity beyond pairwise correlations. Across all disciplines, the reliability and completeness of structural data are an important issue. In the case of brain networks on the level of cortical areas (or connectomes), one issue is whether or not to regard these networks as weighted or unweighted graphs [32,257]. Furthermore, most systems for which such correlations are of interest will have some form of multiscale organization [258]. Hence, any analysis on SC/FC relationships will require selecting suitable spatial and temporal scales. On some level, we can furthermore expect that the structural network (often thought of as 'static' in the context of SC/FC correlations) will also change with time, though often on a longer timescale than functional connectivity. We can furthermore envision a coevolution of structural and functional connectivity towards jointly ensuring a reliable functioning of the system [50].

Even the small discussion of the plausibility of these stylized forms of dynamics in the context of the application domains shown in figure 1 illustrates how real-life complex systems contain a range of dynamical usages (functional activity patterns) of a given infrastructure (structural connectivity). It is less clear, however, that even a form of dynamics, which by definition seems to favour one type of functional connectivity (sequential activation for excitable dynamics; synchronous activity for coupled oscillators) can display strong SC/FC signals for the other type of functional connectivity, if the constellations of network architecture, coupling

and dynamical parameters are right. This point is illustrated with the numerical simulations discussed here.

We believe that subsequent investigations might employ the pattern of SC/FC correlations as a means of identifying from a given network structure, which type of dynamics is most plausible, i.e. which type of dynamics this network was 'built for'. Our current understanding of dynamics on networks does not yet allow for such a detailed assessment.

Another direction of extending our investigation is to have continuous chaotic systems. Here, the Lorenz system [259,260], Rössler system [261,262] or Stuart-Landau system [263,264] would be suitable candidates. The question is then, how the results described above change when going from discrete to continuous time and when going from a one-dimensional system (at each node) to a higher-dimensional system. As we have shown above, in the case of excitable dynamics, the step from discrete to continuous time leaves the results qualitatively intact, as does the step from a one-dimensional to a two-dimensional system in the case of regular oscillations. For chaotic systems, this needs to be investigated in detail.

Complex behaviour (patterns with long-range correlations, in contrast to chaotic dynamics without order on a larger scale) can emerge near critical points. Given our hypothesis that high SC/FC$_{seq}$ is associated with large-scale patterns (e.g. excitation waves [20]), the distinction between chaotic and complex behaviour may have a strong effect on SC/FC correlations. This aspect requires further investigation and coupled electronic chaotic oscillators may be an interesting test case for this, as they provide a high level of realism, in particular for brain dynamics, together with a detailed understanding of their collective behaviours [265,266]. Electronic chaotic oscillators can be used as a physical model of brain dynamics [265,266] as similar dynamics to neuronal activity are observed in such networks of diffusively coupled single-transistor oscillators.

Seeing sequential activation as a proxy of large-scale patterns certainly has its limitations. In particular, we expect that criticality—power-law distributions of activity and long-range correlations that have been studied in great detail in general networks [267,268] and in particular in brain dynamics [27,269–271]—cannot be identified in this way.

On the technical level, various definitions of co-activation and sequential activation are plausible, e.g. different normalizations, time delays and discretizations. We did not explore these aspects in detail. A discussion of the impact of these aspects can be found for example in [30,50].

As often with numerical investigations, some seemingly small 'design decisions' affect the results. In the SER model, for example, near the deterministic limit, longer runs do not provide more information, as the system rapidly settles into a (periodic) attractor. Then, only a large number of short runs can reveal the underlying network architecture. The same is true for phase oscillators, which provided the coupling is high enough given a certain spread of eigenfrequencies, rapidly settle into a fully synchronized state no longer informative about the architecture of the network. Here also, transients from many runs need to be collected.

In the case of coupled phase oscillators, delayed coupling [272,273] and phase shift coupling [274] can alter the synchronization properties and the dynamical behaviour dramatically. In the case of time delays, we can expect that strength is shifted between co-activation and sequential activation. Time delays are presumed to be a key ingredient in reproducing realistic neural dynamics [187,275,276]. Phase shift coupling, on the

other hand, can transform phase oscillators into excitable units [274]. These points, together with our observation that the exact form of the coupling is relevant for the behaviour of SC/FC correlations, underlines that even for the simple models discussed here more investigations are necessary.

With our investigations, we set out to understand which network features and which class of dynamics rather enhance SC/FC$_{\text{sim}}$ or rather enhance SC/FC$_{\text{seq}}$. As a rule, we find that modularity enhances SC/FC$_{\text{sim}}$, while broad degree distribution or randomness enhances SC/FC$_{\text{seq}}$. Increase in coupling favours high SC/FC$_{\text{sim}}$, while high parameter diversity tends to enhance SC/FC$_{\text{seq}}$.

From the view of dynamics, excitation models tend to favour FC$_{\text{seq}}$, a trend we observe both with the minimal (SER) model of the excitable dynamics and with the more realistic FitzHugh–Nagumo model. By contrast, regular oscillators favour FC$_{\text{sim}}$, as we see with the stylized (coupled phase oscillator) model and, at a higher level of realism, with the FitzHugh–Nagumo model in its oscillatory regime. In the case of the chaotic oscillators, the choice of the coupling term used here leads to a persistent dominance of high positive SC/FC$_{\text{seq}}$, but for a complete view about the SC/FC strengths further investigation with other types of coupling is needed.

The conceptualization of the synchronous and sequential activity in different application scenarios is more sophisticated than in the case of minimal models, which indicates that broader definitions of the two notions are needed. However, as we show in the second half of our investigation, the systematics extracted from investigating minimal models help us better organize the diverse findings in the application domains and thus provides a fresh perspective on dynamical processes in network-like systems in these fields. Specifically, we argue that FC$_{\text{sim}}$ is associated with simultaneous measurements either of the dynamical activity of nodes or of links, where the concept of 'simultaneous events' introduces a timescale, at which events are considered to be 'synchronous'. Relatedly, in terms of a more general view on FC$_{\text{seq}}$, we argue that it can be seen as flow of information or materials in the system, summarizing concepts such as influence and diffusion.

5. Methods

5.1. Network topologies

The simulations were performed on a set of abstract graphs (modular, Erdős-Rényi, Barabási-Albert, Newman–Watts–Strogatz and hierarchical [277]) and three real-life networks (neural [32], social [34], metabolic [33]). The description of the network architectures of the graphs is given below:

Modular graph: includes 60 nodes and has density 0.23. Each graph is constructed by starting from four cliques, in which every node is linked with all the other nodes in the same clique. Then, edges are randomly rewired with probability $p = 0.23$ to link different cliques.

Watts–Strogatz graph: includes 60 nodes and every node of the graph is linked with its 15 nearest neighbours in a ring topology [278].

Erdős-Rényi (ER) graph: includes 60 nodes and the probability of edge creation for each node is 0.23 [279].

Barabási-Albert (BA) graph: Each BA graph consists of 60 nodes and it is grown by attaching new nodes, each with 8 edges that are preferentially attached to existing nodes with high degree [280].

Hierarchical graph: includes 64 nodes, 174 edges and it has a scale-free topology with modular structure. The detailed construction process is described in [277].

Neural graph: includes 89 nodes (cortical areas) and 676 edges derived via thresholding and symmetrization from the 29×91 connectivity matrix (inter-areal connection strength measurements) described in [32]. An edge between two nodes is accepted if the decimal logarithm of the corresponding connection strength measurement is above the threshold value 10^{-3} (see electronic supplementary material for more details).

Metabolic graph: includes 72 nodes (metabolites) and 486 edges [33]. We use the systems biology markup language (SBML) model 'e-coli-core' from the BIGG database (bigg.ucsd.edu) and extract the stoichiometric matrix S. The adjacency matrix of the metabolite-centric metabolic network shown in figure 1 is then obtained by mapping all non-zero entries in SS^T to 1, where S^T is the transpose of S.

Social graph: includes 77 nodes (people) and 875 edges [34]. It is an undirected graph and an edge between two nodes is created, if one's knowledge about the skills of others within the company exceeds a threshold equal to 5.0 (see electronic supplementary material for more details about the real-life networks).

5.2. Topological changes

In the first instance, three initial graphs that have distinct structure were randomized or rewired in different proportions, such as the ratio No Changes/No Edges $\simeq 0.11$ corresponds to a percentage of 10% of randomization/rewiring process. Thus, for the modular and the regular graph every 10% of randomization/rewiring process corresponds to 50 swaps/rewiring changes of edges. The degree of the nodes is preserved and only the structure of the network changes. For the hierarchical graph, 20 swaps of the edges for every 10% of randomization are enough to end up with a scale-free graph, whose modularity is completely destroyed. As a consequence, the randomized network retains its degree distribution and the presence of hubs, but without the embedded modularity that it initially had, similar to a scale-free topology as the preferential attachment model from [280]. The modular and the hierarchical networks were randomized, according to the Markov chain algorithm [281]: pairs of randomly selected edges are swapped, providing no self-loop or multiple edges between two nodes are created. The rewiring process was performed on the Watts–Strogatz model according to the scheme from [278]: a randomly selected link was destroyed and a new one was created between one of the two nodes and a randomly selected one; the requirement of self-loops and multiple edges between two nodes must be, also, satisfied. During the rewiring process and before we end up with an Erdős–Rényi graph, the network passes through a 'small world' regime [278].

5.3. SER model

The models we used to highlight the two classes of functional connectivity cover a range of different types of dynamical processes: excitable dynamics, regular oscillations and chaotic oscillations. The SER model, a simple cellular automaton model of excitable dynamics, acts on discrete time and the update rules are simultaneously applied as follows to go from the state at time t to the state at time $t + 1$: (1) A node in the susceptible state (S) changes into a node in the state of the excited nodes (E) if one or more of its neighbours are excited. Alternatively, a node can go from S to E in a stochastic way with a given (usually small) rate of spontaneous excitation, f. (2) A node in the excited state (E) changes into a node in the refractory state (R). (3) A node in the refractory state (R) changes into a node in the susceptible state (S) in a stochastic way with a given refractory probability p. This model has been originally studied as a model of self-organized criticality [282] and later been applied to address abstract questions of

excitable dynamics on graphs [29,31,283], as well as topics in neuroscience [19,50]. In the deterministic limit, $p = 1$, $f = 0$, the contribution of the three cycles significantly affects the collective dynamics [28,30]. Due to its discreteness in time and states, in the SER model co-activity and sequential activity of the nodes can be defined in a parameter-free way: each node can be found in one of the three states $x_i(t) \in \{S, E, R\}$, however, in the analysis of SC/FC relationships we only distinguish two states:

$$c_i(t) = \begin{cases} 1 & x_i(t) = E \\ 0 & x_i(t) = S \text{ or } R. \end{cases}$$

Separating the nodes into the two categories (active or inactive) is a convenient way to define the two classes of functional connectivity. The co-activation matrix is

$$C_{ij} = \sum_t c_i(t)c_j(t),$$

and the sequential activation matrix is

$$S_{ij} = \sum_t c_i(t)c_j(t-1).$$

It should be noted that different normalizations of these quantities can be envisioned (see [28] for a detailed discussion).

For all the cases where the SER model was used, we simulated $N_R = 10\,000$ runs of $t_{\max} = 10$ (unit timestep) with randomly generated initial conditions, with 6% of the nodes to be in the E state and the rest to be in S or R state with an equiprobability. The information for the FC matrices was accumulated by initially taking the sum over the time of each matrix, and then by taking the sum over the multiple runs. The SC/FC correlations were computed with the Pearson correlation between the flattened adjacency and the co-activation/sequential activation matrix. The final average value was computed as the mean of the correlations from the 10 different initial graphs, and the errors as the standard deviation of these correlation values. We obtain the main results using the recovery probability $p = 0.1$ and transmission probability $f = 0.001$.

5.4. Phase oscillators

The second, also well studied, model studied here is the Kuramoto model [118,284]. It describes the behaviour of a large set of coupled phase oscillators and their transition to synchronization. We use it here in a variant, where the oscillators are coupled according to the architecture of a given network [24]. Each of the oscillators has an intrinsic natural frequency (or 'eigenfrequency') ω_i and all of them are equally coupled with their neighbours with coupling k. The evolution of the phase of a node in a population of N oscillators is governed by the following dynamics:

$$\frac{\mathrm{d}\theta_i}{\mathrm{d}t} = \omega_i + \frac{k}{N}\sum_{j=1}^{N} A_{ij}\sin(\theta_j - \theta_i), \quad i = 1, \ldots, N.$$

This model has been instrumental in the past for understanding how network topology determines synchronizability [23] and how synchronization patterns emerge from architectural features of networks [22].

Investigating the behaviour of the two classes of FC, in this model, requires oscillators that have not reached the total synchronization, which indicates the absolute 'win' of the co-activation. Thus, Gaussian noise, scaled by amplitude σ, was added in order to delay the synchronization process.

$$\frac{\mathrm{d}\theta_i}{\mathrm{d}t} = \omega_i + \frac{k}{N}\sum_{j=1}^{N} A_{ij}\sin(\theta_j - \theta_i) + \sigma u, \quad i = 1, \ldots, N$$

The matrix of functional connectivity, in this case, is constructed from the correlation coefficient between the time series

of the *effective frequency*:

$$C_{ij}(\delta t) = \mathrm{corr}_t(\Omega_i(t), \Omega_j(t + \delta t)), \quad (5.1)$$

where

$$\Omega_i(t) = \langle \Delta\theta_i(t)\rangle_t = \frac{1}{2\Delta t}\sum_{t'=t-\Delta t}^{t+\Delta t-1} \theta_i(t'+1) - \theta_i(t')$$

for some suitable choice of a time window Δt.

For a continuous model, such as the coupled phase oscillators, the definition of the two classes of functional connectivity is not possible in a parameter-free manner. In equation (5.1), for $\delta t = 0$, we have strict co-activation and with increasing time lag δt a transition from correlations dominated by co-activation to correlations dominated by sequential activation (before the two timeseries of effective frequencies essentially de-couple). Particularly, the decision of the appropriate selection of the time lag for the sequential activation was based on the results of SC/FC correlations as a function of the coupling strength for different values of time lag. In the electronic supplementary material, figure S5 shows the multiple curves of the different time delay values for a modular and an ER graph. While the effect of the increasing time delay in a modular graph is the gradual decrease of the SC/FC correlation, in the ER graph three groups of curves emerge. The first one corresponds to the co-activity of the nodes (includes the zero and time lag equal to 1), the second group includes the curve that corresponds to the time-delay 2 and, in this case, is the appropriate selection for the sequential activation, since larger values for the time delay, which constitutes the third group of curves, have zero contribution in the sequential activation.

For this case, we simulated $N_R = 100$ runs over $t_{\max} = 50$ using the Euler method, with randomly generated initial conditions from the uniform distribution $(-\pi, \pi)$ on different graphs with non-identical oscillators. The integration timestep for the solution of the system was equal to 0.1. The Gaussian noise was selected to have zero mean, unit variance and it was scaled by amplitude $\sigma = 0.25$. The eigenfrequencies were uniformly selected from the interval $(0, 1)$. The size of the time window we selected Δt for the effective frequency was equal to 20 and the FC matrices were constructed from the Pearson correlation of the effective frequencies between each pair of nodes. The diagonal elements are zero, by default. As in the SER model, the SC/FC correlations were computed with the Pearson correlation of the flattened adjacency and FC matrices. For the latter one, the sum, over multiple runs, was taken and the average correlation values derived from the SC/FC correlations of 10 different initial networks; the corresponding errors derived from the standard deviation of these 10 values. For the main results, we selected a coupling strength equal to 10.

5.5. Logistic map

The third model that was used as a dynamical probe of network architectures is the logistic map. Such dimensional maps (also termed finite-difference equations or recursion relations) are used to describe the evolution of one variable over discrete steps in time, following a template of the form $x_{t+1} = f(x_t)$. The logistic map

$$x_{t+1} = Rx_t(1 - x_t)$$

is the most well-known example of this class of dynamical models [285]. Starting from a stable fixed point at low R, the system undergoes a sequence of period-doubling bifurcations with increasing R leading to a large regime of deterministic chaos, occasionally interrupted by small periodic windows. Systems of coupled logistic maps have been studied extensively as a model for spatio-temporal pattern formation [286] and on networks [51,52,287].

The coupled system has the form

$$x_i(t+1) = R_i x_i(t)(1 - x_i(t)) + \frac{k}{N} \sum_{j=1}^{N} A_{ij}(x_j(t) - x_i(t)),$$

$$i = 1, \ldots, N,$$

where k is the coupling strength and A_{ij} is the network's adjacency matrix (structural connectivity). Note that we impose additional constraints on the system to force each $x_i(t)$ to be in the interval $x \in [0, 1]$. We define FC as the correlation between the timeseries of the nodes for zero time lag (co-activation) and a time lag of 1 (sequential activation):

$$C_{ij} = \text{corr}_t(x_i(t), x_j(t)), \quad S_{ij} = \text{corr}_t(x_i(t), x_j(t+1)).$$

We simulated $N_R = 50$ runs over $t_{\max} = 500$ (unit timestep) with randomly generated initial conditions from the uniform distribution $(0, 1)$. The parameter R was randomly selected by each oscillator from the interval $(3.7, 3.9)$. For the main results, the coupling strength that was used was equal to 2. The FC matrices were constructed from the Pearson correlation between the time series of the x variable (diagonal elements are zero by default). The SC/FC correlations derived from the comparison of the flattened adjacency and FC matrices, by taking the Pearson correlation, after each run. The average correlation value derived from the mean correlation values over the multiple runs and the errors from the standard deviation of the correlation values over the multiple runs.

5.6. FitzHugh–Nagumo model

As a more sophisticated model of excitable dynamics and regular oscillations, we use the FitzHugh–Nagumo model [288,289], a two-dimensional model of ordinary differential equations (ODEs).

The FitzHugh–Nagumo model is composed of two coupled variables, where x represents the membrane potential and y is the recovery variable:

$$\tau_x \frac{\partial x_i(t)}{\partial t} = \gamma x_i(t) - \frac{x_i^3(t)}{3} - y_i(t) + \frac{k}{\langle d \rangle} \sum_j A_{ij}[x_j(t) - x_i(t)] + \sigma v_x$$

and

$$\tau_y \frac{\partial y_i(t)}{\partial t} = x_i(t) - \beta y_i(t) + a,$$

where $\langle d \rangle$ is the average degree in the network, τ_x, τ_y are the timescale parameters for each variable, again k the coupling strength among the connected nodes, v_x, v_y are random variables drawn from a Gaussian distribution of zero mean and unit variance and σ the amplitude of the noise. In the xy plane, we can distinguish three regions and the intersection of the nullclines of the system (see electronic supplementary material, figure S1), $\partial x_i(t)/\partial t = 0 \wedge \partial y_i(t)/\partial t = 0$ defines the fixed point. Hence, depending on the region that the fixed point is placed, the system can be found either in the oscillatory or in the excitable regime. By shifting the linear nullcline (changing the parameter a), we can move from region 1 (excitable regime) to region 2 (oscillatory regime). Here, we plot the correlation values during the randomization process of a modular graph in the excitable and in the oscillatory regime.

As with the logistic map, coupled FitzHugh–Nagumo oscillators have been employed in a range of investigations focusing on spatio-temporal pattern formation [290] and collective dynamics in networks [26].

We simulated 10 runs, using the Euler method to solve the system. The total time of each simulated run was 180 s and the integration step 0.1 ms. We downsampled the output at 1 ms and we used this to calculate the FC. The FC_{sim} matrix derived from the sum of the co-activation matrices over the time of each run. The co-activation matrices were constructed as in the SER model, after discretizing the time series (spike detection) with a threshold equal to one and using a time window equal to 1 ms. For the FC_{seq} matrices, various widths of time windows were selected in order to discretize the time series and detect the spikes. Larger time windows include both spikes that occur simultaneously and sequentially, thus, from the whole activity within the window, the co-activity (time window 1 ms) was subtracted. The calculation of SC/FC correlations derived from the flattened adjacency and functional connectivity matrices, after excluding the diagonal elements. The final correlation values came from the mean value of the 10 correlation values from the different runs and the errors from the corresponding standard deviation. The co-activity of the nodes, as well as the sequential activity of the nodes, using different window sizes, were tested under different values for the coupling strength and the noise amplitude for both the excitable ($a = 0.8$) and oscillatory regime ($a = 0$) (see electronic supplementary material, S6). The selected parameter values for the system are $\beta = 0.6$, $\gamma = 1$, $\tau_x = 0.001$, $\tau_y = 0.1$. The random numbers for the noise u_x were selected from a normal distribution with zero mean and unit variance, whose amplitudes were scaled by σ and with an additional scaling parameter $\sqrt{dt/\tau_x}$ (dt is the size of the integration step). The scaling term for the u_y is equal to zero. For the main results, we selected the coupling strength (divided by the average degree in the network) equal to 0.044, the amplitude of the noise equal to $\sigma = 0.15$ and the time window of 12 ms for the sequential activation.

References

1. Mukherjee S, Speed TP. 2008 Network inference using informative priors. *Proc. Natl Acad. Sci. USA* **105**, 14 313–14 318. (doi:10.1073/pnas.0802272105)

2. Marbach D, Prill RJ, Schaffter T, Mattiussi C, Floreano D, Stolovitzky G. 2010 Revealing strengths and weaknesses of methods for gene network inference. *Proc. Natl Acad. Sci. USA* **107**, 6286–6291. (doi:10.1073/pnas.0913357107)

3.   Marbach D *et al.* 2012 Wisdom of crowds for robust gene network inference. *Nat. Methods* **9**, 796–804. (doi:10.1038/nmeth.2016)

4.   Zhao J, Zhou Y, Zhang X, Chen L. 2016 Part mutual information for quantifying direct associations in networks. *Proc. Natl Acad. Sci. USA* **113**, 5130–5135. (doi:10.1073/pnas.1522586113)

5.   Newman MEJ. 2018 Network structure from rich but noisy data. *Nat. Phys.* **14**, 542–545. (doi:10.1038/s41567-018-0076-1)

6.   Honey CJ, Sporns O, Cammoun L, Gigandet X, Thiran J-P, Meuli R, Hagmann P. 2009 Predicting human resting-state functional connectivity from structural connectivity. *Proc. Natl Acad. Sci. USA* **106**, 2035–2040. (doi:10.1073/pnas.0811168106)

7.   Sonnenschein N, Dzib JFG, Lesne A, Eilebrecht S, Boulkroun S, Zennaro M-C, Benecke A, Hütt M-T. 2012 A network perspective on metabolic inconsistency. *BMC Syst. Biol.* **6**, 41. (doi:10.1186/1752-0509-6-41)

8.   Ideker T, Krogan NJ. 2012 Differential network biology. *Mol. Syst. Biol.* **8**, 565. (doi:10.1038/msb.2011.99)

9.   Dong Y, Zha Q, Zhang H, Kou G, Fujita H, Chiclana F, Herrera-Viedma E. 2018 Consensus reaching in social network group decision making: research paradigms and challenges. *Knowledge-Based Syst.* **162**, 3–13. (doi:10.1016/j.knosys.2018.06.036)

10. Jalili M. 2013 Social power and opinion formation in complex networks. *Physica A* **392**, 959–966. (doi:10.1016/j.physa.2012.10.013)

11. Potts R, Vella K, Dale A, Sipe N. 2016 Exploring the usefulness of structural–functional approaches to analyse governance of planning systems. *Planning Theory* **15**, 162–189. (doi:10.1177/1473095214553519)

12. Wainwright J, Turnbull L, Ibrahim TG, Lexartza-Artza I, Thornton SF, Brazier RE. 2011 Linking environmental regimes, space and time: interpretations of structural and functional connectivity. *Geomorphology* **126**, 387–404. (doi:10.1016/j.geomorph.2010.07.027)

13. Baartman JEM *et al.* 2020 What do models tell us about water and sediment connectivity? *Geomorphology* **367**, 107300. (doi:10.1016/j.geomorph.2020.107300)

14. Wohl E *et al.* 2019 Connectivity as an emergent property of geomorphic systems. *Earth Surf. Processes Landforms* **44**, 4–26. (doi:10.1002/esp.4434)

15. Boguna M, Krioukov D, Claffy KC. 2009 Navigability of complex networks. *Nat. Phys.* **5**, 74–80. (doi:10.1038/nphys1130)

16. Meyer M, Hütt M-T, Bendul JC. 2015 The elementary flux modes of a manufacturing system: a novel approach to explore the relationship of network structure and function. *Int. J. Prod. Res.* **54**, 16. (doi:10.1080/00207543.2015.1106612)

17. Li Y, Tao F, Cheng Y, Zhang X, Nee AYC. 2017 Complex networks in advanced manufacturing systems. *J. Manuf. Syst.* **43**, 409–421. (doi:10.1016/j.jmsy.2016.12.001)

18. Zhang J, Zhang Y, Wang L, Sang L, Yang J, Yan R, Li P, Wang J, Qiu M. 2017 Disrupted structural and functional connectivity networks in ischemic stroke patients. *Neuroscience* **364**, 212–225. (doi:10.1016/j.neuroscience.2017.09.009)

19. Müller-Linow M, Hilgetag CC, Hütt M-T. 2008 Organization of excitable dynamics in hierarchical biological networks. *PLoS Comput. Biol.* **4**, e1000190. (doi:10.1371/journal.pcbi.1000190)

20. Moretti P, Hütt M-T. 2020 Link-usage asymmetry and collective patterns emerging from rich-club organization of complex networks. *Proc. Natl Acad. Sci. USA* **117**, 18332–18340. (doi:10.1073/pnas.1919785117)

21. Turnbull L *et al.* 2018 Connectivity and complex systems: learning from a multi-disciplinary perspective. *Appl. Netw. Sci.* **3**, 1–49. (doi:10.1007/s41109-018-0067-2)

22. Arenas A, Diaz-Guilera A, Pérez-Vicente CJ. 2006 Synchronization reveals topological scales in complex networks. *Phys. Rev. Lett.* **96**, 114102. (doi:10.1103/PhysRevLett.96.114102)

23. Arenas A, Díaz-Guilera A, Kurths J, Moreno Y, Zhou C. 2008 Synchronization in complex networks. *Phys. Rep.* **469**, 93–153. (doi:10.1016/j.physrep.2008.09.002)

24. Rodrigues FA, D.M. Peron TK, Ji P, Kurths J. 2016 The Kuramoto model in complex networks. *Phys. Rep.* **610**, 1–98. (doi:10.1016/j.physrep.2015.10.008)

25. Chen M, Shang Y, Zhou C, Wu Y, Kurths J. 2009 Enhanced synchronizability in scale-free networks. *Chaos* **19**, 013105. (doi:10.1063/1.3062864)

26. Messé A, Hütt M-T, König P, Hilgetag CC. 2015 A closer look at the apparent correlation of structural and functional connectivity in excitable neural networks. *Sci. Rep.* **5**, 1–5. (doi:10.1038/srep07870)

27. Haimovici A, Tagliazucchi E, Balenzuela P, Chialvo DR. 2013 Brain organization into resting state networks emerges at criticality on a model of the human connectome. *Phys. Rev. Lett.* **110**, 178101. (doi:10.1103/PhysRevLett.110.178101)

28. Garcia GC, Lesne A, Hütt M-T, Hilgetag CC. 2012 Building blocks of self-sustained activity in a simple deterministic model of excitable neural networks. *Front. Comput. Neurosci.* **6**, 50. (doi:10.3389/fncom.2012.00050)

29. Fretter C, Lesne A, Hilgetag CC, Hütt M-T. 2017 Topological determinants of self-sustained activity in a simple model of excitable dynamics on graphs. *Sci. Rep.* **7**, 42340. (doi:10.1038/srep42340)

30. Messé A, Hütt M-T, Hilgetag CC. 2018 Toward a theory of coactivation patterns in excitable neural networks. *PLoS Comput. Biol.* **14**, e1006084. (doi:10.1371/journal.pcbi.1006084)

31. Garcia GC, Lesne A, Hilgetag CC, Hütt M-T. 2014 Role of long cycles in excitable dynamics on graphs. *Phys. Rev. E* **90**, 52805. (doi:10.1103/PhysRevE.90.052805)

32. Markov NT *et al.* 2014 A weighted and directed interareal connectivity matrix for macaque cerebral cortex. *Cereb. Cortex* **24**, 17–36. (doi:10.1093/cercor/bhs270)

33. Palsson B. 2015 *Systems biology*. Cambridge, UK: Cambridge University Press.

34. Cross RL, Cross RL, Parker A. 2004 *The hidden power of social networks: understanding how work really gets done in organizations*. Boston, MA: Harvard Business Review Press.

35. Wu Z, Guo A. 1999 Selective visual attention in a neurocomputational model of phase oscillators. *Biol. Cybern.* **80**, 205–214. (doi:10.1007/s004220050518)

36. Corchs S, Deco G. 2001 A neurodynamical model for selective visual attention using oscillators. *Neural Netw.* **14**, 981–990. (doi:10.1016/S0893-6080(01)00055-7)

37. Messé A, Rudrauf D, Benali H, Marrelec G. 2014 Relating structure and function in the human brain: relative contributions of anatomy, stationary dynamics, and non-stationarities. *PLoS Comput. Biol.* **10**, e1003530. (doi:10.1371/journal.pcbi.1003530)

38. Babloyantz A, Lourenço C. 1994 Computation with chaos: a paradigm for cortical activity. *Proc. Natl Acad. Sci. USA* **91**, 9027–9031. (doi:10.1073/pnas.91.19.9027)

39. Xu K, Maidana JP, Castro S, Orio P. 2018 Synchronization transition in neuronal networks composed of chaotic or non-chaotic oscillators. *Sci. Rep.* **8**, 1–12. (doi:10.1038/s41598-018-26730-9)

40. Becker T, Beber ME, Windt K, Hütt M-T, Helbing D. 2011 Flow control by periodic devices: a unifying language for the description of traffic, production, and metabolic systems. *J. Stat. Mech: Theory Exp.* **2011**, P05004. (doi:10.1088/1742-5468/2011/05/P05004)

41. Camacho D, De La Fuente A, Mendes P. 2005 The origin of correlations in metabolomics data. *Metabolomics* **1**, 53–63. (doi:10.1007/s11306-005-1107-3)

42. Müller-Linow M, Weckwerth W, Hütt M-T. 2007 Consistency analysis of metabolic correlation networks. *BMC Syst. Biol.* **1**, 1–12. (doi:10.1186/1752-0509-1-1)

43. Kumar S, D'Souza RN, Corno M, Ullrich MS, Kuhnert N, Hütt M-T. 2020 Correlation network analysis based on untargeted LC-MS profiles of cocoa reveals processing stage and origin country. *bioRxiv*. (doi:10.1101/2020.02.09.940585)

44. Moreno Y, Nekovee M, Pacheco AF. 2004 Dynamics of rumor spreading in complex networks. *Phys. Rev. E* **69**, 066130. (doi:10.1103/PhysRevE.69.066130)

45. Helbing D. 2012 *Social self-organization: agent-based simulations and experiments to study emergent social behavior*. New York, NY: Springer.

46. Nowak AK, Vallacher RR, R.Praszkier, Rychwalska A, Zochowski M. 2020 Synchronization in groups and societies. In *In sync: the emergence of function in minds, groups and societies (understanding complex systems)*, pp. 113–136. New York, NY: Springer.

47. Dooley KJ, Van de Ven AH. 1999 Explaining complex organizational dynamics. *Organ. Sci.* **10**, 358–372. (doi:10.1287/orsc.10.3.358)

48. Whitby S, Parker D, Tobias A. 2001 Non-linear dynamics and duopolistic competition: a R&D model and simulation. *J. Bus. Res.* **51**, 179–191. (doi:10.1016/S0148-2963(99)00050-8)

49. Yuan X, Nishant R. 2019 Understanding the complex relationship between R&D investment and firm growth: a chaos perspective. *J. Bus. Res.* **129**, 666–678. (doi:10.1016/j.jbusres.2019.11.043)

50. Damicelli F, Hilgetag CC, Hütt M-T, Messé A. 2019 Topological reinforcement as a principle of modularity emergence in brain networks. *Netw. Neurosci.* **3**, 589–605. (doi:10.1162/netn_a_00085)

51. Lind PG, Gallas JAC, Herrmann HJ. 2004 Coherence in scale-free networks of chaotic maps. *Phys. Rev. E* **70**, 056207. (doi:10.1103/PhysRevE.70.056207)

52. Masoller C, Atay FM. 2011 Complex transitions to synchronization in delay-coupled networks of logistic maps. *Eur. Phys. J. D* **62**, 119–126. (doi:10.1140/epjd/e2011-10370-7)

53. Hütt M-T, Jain MK, Hilgetag CC, Lesne A. 2012 Stochastic resonance in discrete excitable dynamics on graphs. *Chaos, Solitons & Fractals* **45**, 611–618. (doi:10.1016/j.chaos.2011.12.011)

54. Prell C. 2012 *Social network analysis: history, theory and methodology*. Los Angeles, CA: Sage.

55. Klamt S, Haus U-U, Theis F. 2009 Hypergraphs and cellular networks. *PLoS Comput. Biol.* **5**, e1000385. (doi:10.1371/journal.pcbi.1000385)

56. Battiston F, Cencetti G, Iacopini I, Latora V, Lucas M, Patania A, Young J-G, Petri G. 2020 Networks beyond pairwise interactions: structure and dynamics. *Phys. Rep.* **874**, 1–92. (doi:10.1016/j.physrep.2020.05.004)

57. Gorochowski TE, Bernardo MD, Grierson CS. 2012 Evolving dynamical networks: a formalism for describing complex systems. *Complexity* **17**, 18–25. (doi:10.1002/cplx.20386)

58. Maslennikov OV, Nekorkin VI. 2017 Adaptive dynamical networks. *Phys. Usp.* **60**, 694. (doi:10.3367/UFNe.2016.10.037902)

59. Battaglia D et al. 2020 Dynamic functional connectivity between order and randomness and its evolution across the human adult lifespan. *NeuroImage* **222**, 117156. (doi:10.1016/j.neuroimage.2020.117156)

60. Nunes JP, Wainwright J, Bielders CL, Darboux F, Fiener P, Finger D, Turnbull L. 2018 Better models are more effectively connected models. *Earth Surf. Processes Landforms* **43**, 1355–1360. (doi:10.1002/esp.4323)

61. Erős T, Olden JD, Schick RS, Schmera D, Fortin M. 2012 Characterizing connectivity relationships in freshwaters using patch-based graphs. *Landsc. Ecol.* **27**, 303–317. (doi:10.1007/s10980-011-9659-2)

62. Schick RS, Lindley ST. 2007 Directed connectivity among fish populations in a riverine network. *J. Appl. Ecol.* **44**, 1116–1126. (doi:10.1111/j.1365-2664.2007.01383.x)

63. Marra WA, Kleinhans MG, Addink EA. 2014 Network concepts to describe channel importance and change in multichannel systems: test results for the Jamuna river, Bangladesh. *Earth Surf. Processes Landforms* **39**, 766–778. (doi:10.1002/esp.3482)

64. Tejedor A, Longjas A, Zaliapin I, Foufoula-Georgiou E. 2015 Delta channel networks: 1. A graph-theoretic approach for studying connectivity and steady state transport on deltaic surfaces. *Water Resour. Res.* **51**, 3998–4018. (doi:10.1002/2014WR016577)

65. Passalacqua P. 2017 The delta connectome: a network-based framework for studying connectivity in river deltas. *Geomorphology* **277**, 50–62. (doi:10.1016/j.geomorph.2016.04.001)

66. Pearson SG, van Prooijen BC, Elias EPL, Vitousek S, Wang ZB. 2020 Sediment connectivity: a framework for analyzing coastal sediment transport pathways. *J. Geophys. Res.: Earth Surface* **125**, e2020JF005595. (doi:10.1029/2020JF005595)

67. Trigg MA, Michaelides K, Neal JC, Bates PD. 2013 Surface water connectivity dynamics of a large scale extreme flood. *J. Hydrol.* **505**, 138–149. (doi:10.1016/j.jhydrol.2013.09.035)

68. Abed-Elmdoust A, Singh A, Yang Z-L. 2017 Emergent spectral properties of river network topology: an optimal channel network approach. *Sci. Rep.* **7**, 1–9. (doi:10.1038/s41598-017-11579-1)

69. Rigon R, Rinaldo A, Rodriguez-Iturbe I, Bras RL, Ijjasz-Vasquez E. 1993 Optimal channel networks: a framework for the study of river basin morphology. *Water Resour. Res.* **29**, 1635–1646. (doi:10.1029/92WR02985)

70. Balister P, Balogh J, Bertuzzo E, Bollobás B, Caldarelli G, Maritan A, Mastrandrea R, Morris R, Rinaldo A. 2018 River landscapes and optimal channel networks. *Proc. Natl Acad. Sci. USA* **115**, 6548–6553. (doi:10.1073/pnas.1804484115)

71. Jencso KG, McGlynn BL, Gooseff MN, Wondzell SM, Bencala KE, Marshall LA. 2009 Hydrologic connectivity between landscapes and streams: transferring reach- and plot-scale understanding to the catchment scale. *Water Resour. Res.* **45**, W04428. (doi:10.1029/2008WR007225)

72. Turnbull L, Wainwright J. 2019 From structure to function: understanding shrub encroachment in drylands using hydrological and sediment connectivity. *Ecol. Indic.* **98**, 608–618. (doi:10.1016/j.ecolind.2018.11.039)

73. Rinderer M, Ali G, Larsen LG. 2018 Assessing structural, functional and effective hydrologic connectivity with brain neuroscience methods: state-of-the-art and research directions. *Earth Sci. Rev.* **178**, 29–47. (doi:10.1016/j.earscirev.2018.01.009)

74. Turnbull L, Wainwright J, Brazier RE. 2010 Changes in hydrology and erosion over a transition from grassland to shrubland. *Hydrol. Process.: An Int. J.* **24**, 393–414. (doi:10.1002/hyp.7491)

75. Phillips RW, Spence C, Pomeroy JW. 2011 Connectivity and runoff dynamics in heterogeneous basins. *Hydrol. Processes* **25**, 3061–3075. (doi:10.1002/hyp.8123)

76. Zuecco G, Rinderer M, Penna D, Borga M, van Meerveld HJ. 2019 Quantification of subsurface hydrologic connectivity in four headwater catchments using graph theory. *Sci. Total Environ.* **646**, 1265–1280. (doi:10.1016/j.scitotenv.2018.07.269)

77. Keefer TO, Moran MS, Paige GB. 2008 Long-term meteorological and soil hydrology database, walnut gulch experimental watershed, Arizona, United States. *Water Resour. Res.* **44**, W05S07. (doi:10.1029/2006WR005702)

78. Zaliapin I, Foufoula-Georgiou E, Ghil M. 2010 Transport on river networks: a dynamic tree approach. *J. Geophys. Res.: Earth Surface* **115**, F00A15. (doi:10.1029/2009JF001281)

79. Czuba JA, Foufoula-Georgiou E. 2014 A network-based framework for identifying potential synchronizations and amplifications of sediment delivery in river basins. *Water Resour. Res.* **50**, 3826–3851. (doi:10.1002/2013WR014227)

80. Sánchez-Andrés R, Sánchez-Carrillo S, Ortiz-Llorente MJ, Álvarez-Cobelas M, Cirujano S. 2010 Do changes in flood pulse duration disturb soil carbon dioxide emissions in semi-arid floodplains? *Biogeochemistry* **101**, 257–267. (doi:10.1007/s10533-010-9472-z)

81. Ashauer R, Boxall ABA, Brown CD. 2007 Modeling combined effects of pulsed exposure to carbaryl and chlorpyrifos on *Gammarus pulex*. *Environ. Sci. Technol.* **41**, 5535–5541. (doi:10.1021/es070283w)

82. Parsons AJ, Wainwright J, Abrahams AD, Simanton JR. 1997 Distributed dynamic modelling of interrill overland flow. *Hydrol. Processes* **11**, 1833–1859. (doi:10.1002/(SICI)1099-1085(199711)11:14<1833::AID-HYP499>3.0.CO;2-7)

83. Mueller EN, Wainwright J, Parsons AJ. 2007 Impact of connectivity on the modeling of overland flow within semiarid shrubland environments. *Water Resour. Res.* **43**, W09412. (doi:10.1029/2006WR005006)

84. Korup O. 2005 Large landslides and their effect on sediment flux in south westland, New Zealand. *Earth Surface Process. Landforms: The J. British Geomorphol. Res. Group* **30**, 305–323. (doi:10.1002/esp.1143)

85. Croissant T, Steer P, Lague D, Davy P, Jeandet L, Hilton RG. 2019 Seismic cycles, earthquakes, landslides and sediment fluxes: linking tectonics to surface processes using a reduced-complexity model. *Geomorphology* **339**, 87–103. (doi:10.1016/j.geomorph.2019.04.017)

86. Tunnicliffe J, Brierley G, Fuller IC, Leenman A, Marden M, Peacock D. 2018 Reaction and relaxation in a coarse-grained fluvial system following catchment-wide disturbance. *Geomorphology* **307**, 50–64. (doi:10.1016/j.geomorph.2017.11.006)

87. Betterle A, Schirmer M, Botter G. 2017 Characterizing the spatial correlation of daily streamflows. *Water Resour. Res.* **53**, 1646–1663. (doi:10.1002/2016WR019195)

88. Croke J, Fryirs K, Thompson C. 2013 Channel–floodplain connectivity during an extreme flood event: implications for sediment erosion, deposition, and delivery. *Earth Surf. Processes Landforms* **38**, 1444–1456. (doi:10.1002/esp.3430)

89. Borrett SR, Scharler UM. 2019 Walk partitions of flow in ecological network analysis: review and synthesis of methods and indicators. *Ecol. Indic.* **106**, 105451. (doi:10.1016/j.ecolind.2019.105451)

90. Siqueira T, Durães LD, de Oliveira Roque F. 2014 Predictive modelling of insect metacommunities in biomonitoring of aquatic networks. In *Ecological modelling applied to entomology* (eds C Ferreira, W

Godoy), pp. 109–126. New York, NY: Springer. (doi:10.1007/978-3-319-06877-0_5)

91. Bodin Ö, Saura S. 2010 Ranking individual habitat patches as connectivity providers: integrating network analysis and patch removal experiments. *Ecol. Modell* **221**, 2393–2405. (doi:10.1016/j.ecolmodel.2010.06.017)

92. Erős T, Olden JD, Schick RS, Schmera D, Fortin M-J. 2012 Characterizing connectivity relationships in freshwaters using patch-based graphs. *Landsc. Ecol.* **27**, 303–317. (doi:10.1007/s10980-011-9659-2)

93. Erős T, Lowe WH. 2019 The landscape ecology of rivers: from patch-based to spatial network analyses. *Curr. Landsc. Ecol. Rep.* **4**, 103–112. (doi:10.1007/s40823-019-00044-6)

94. Minor ES, Urban DL. 2008 A graph-theory framework for evaluating landscape connectivity and conservation planning. *Conserv. Biol.* **22**, 297–307. (doi:10.1111/j.1523-1739.2007.00871.x)

95. Bohlen PJ, Groffman PM, Driscoll CT, Fahey TJ, Siccama TG. 2001 Plant–soil–microbial interactions in a northern hardwood forest. *Ecology* **82**, 965–978. (doi:10.1890/0012-9658(2001)082[0965:PSMIIA]2.0.CO;2)

96. Baldan D, Piniewski M, Funk A, Gumpinger C, Flödl P, Höfer S, Hauer C, Hein T. 2020 A multi-scale, integrative modeling framework for setting conservation priorities at the catchment scale for the freshwater pearl mussel *Margaritifera margaritifera*. *Sci. Total Environ.* **718**, 137369. (doi:10.1016/j.scitotenv.2020.137369)

97. Heino J et al. 2017 Integrating dispersal proxies in ecological and environmental research in the freshwater realm. *Environ. Rev.* **25**, 334–349. (doi:10.1139/er-2016-0110)

98. Saura S, Rubio L. 2010 A common currency for the different ways in which patches and links can contribute to habitat availability and connectivity in the landscape. *Ecography* **33**, 523–537. (doi:10.1111/j.1600-0587.2009.05760.x)

99. Schick RS et al. 2008 Understanding movement data and movement processes: current and emerging directions. *Ecol. Lett.* **11**, 1338–1350. (doi:10.1111/j.1461-0248.2008.01249.x)

100. Tonkin JD, Altermatt F, Finn DS, Heino J, Olden JD, Pauls SU, Lytle DA. 2018 The role of dispersal in river network metacommunities: patterns, processes, and pathways. *Freshwater Biol.* **63**, 141–163. (doi:10.1111/fwb.13037)

101. Calabrese JM, Fagan WF. 2004 A comparison-shopper's guide to connectivity metrics. *Front. Ecol. Environ.* **2**, 529–536. (doi:10.1890/1540-9295(2004)002[0529:ACGTCM]2.0.CO;2)

102. Neufeld K, Watkinson DA, Tierney K, Poesch MS. 2018 Incorporating asymmetric movement costs into measures of habitat connectivity to assess impacts of hydrologic alteration to stream fishes. *Divers. Distributions* **24**, 593–604. (doi:10.1111/ddi.12713)

103. Larsen S et al. 2021 The geography of metapopulation synchrony in dendritic river networks. *Ecol. Lett.* **24**, 791–801. (doi:10.1111/ele.13699)

104. Muneepeerakul R, Weitz JS, Levin SA, Rinaldo A, Rodriguez-Iturbe I. 2007 A neutral metapopulation model of biodiversity in river networks. *J. Theor. Biol.* **245**, 351–363. (doi:10.1016/j.jtbi.2006.10.005)

105. Gilarranz LJ, Hastings A, Bascompte J. 2015 Inferring topology from dynamics in spatial networks. *Theor. Ecol.* **8**, 15–21. (doi:10.1007/s12080-014-0231-y)

106. Terui T, Kobayashi S, Okubo Y, Murakami M, Hirose K, Kubo H. 2018 Efficacy and safety of guselkumab, an anti-interleukin 23 monoclonal antibody, for palmoplantar pustulosis: a randomized clinical trial. *JAMA Dermatol.* **154**, 309–316. (doi:10.1001/jamadermatol.2017.5937)

107. Kelly CR, Kahn S, Kashyap P, Laine L, Rubin D, Atreja A, Moore T, Wu G. 2015 Update on fecal microbiota transplantation 2015: indications, methodologies, mechanisms, and outlook. *Gastroenterology* **149**, 223–237. (doi:10.1053/j.gastro.2015.05.008)

108. Holland MD, Hastings A. 2008 Strong effect of dispersal network structure on ecological dynamics. *Nature* **456**, 792–794. (doi:10.1038/nature07395)

109. Bastolla U, Fortuna MA, Pascual-García A, Ferrera A, Luque B, Bascompte J. 2009 The architecture of mutualistic networks minimizes competition and increases biodiversity. *Nature* **458**, 1018–1020. (doi:10.1038/nature07950)

110. Hajian-Forooshani Z, Vandermeer J. 2021 Viewing communities as coupled oscillators: elementary forms from Lotka and Volterra, Kuramoto. *Theor. Ecol.* **14**, 1–8. (doi:10.1007/s12080-020-00493-4)

111. Lotka AJ. 1925 *Elements of physical biology*. Baltimore, MD: Williams & Wilkins.

112. Volterra V. 1926 Variazioni e fluttuazioni del numero d'individui in specie animali conviventi. Memoire della R. Accademia Nazionale dei Lincei, anno CCCCXXIII, II. 1926. (Fluctuations in the abundance of a species considered mathematically). *Nature* **118**, 558-560. (doi:10.1038/118558a0)

113. Brechtel A, Gramlich P, Ritterskamp D, Drossel B, Gross T. 2018 Master stability functions reveal diffusion-driven pattern formation in networks. *Phys. Rev. E* **97**, 032307. (doi:10.1103/PhysRevE.97.032307)

114. Dame RF, Patten BC. 1981 Analysis of energy flows in an intertidal oyster reef. *Mar. Ecol. Progress Ser.* **5**, 115–124. (doi:10.3354/meps005115)

115. Rudolf VHW, Lafferty KD. 2011 Stage structure alters how complexity affects stability of ecological networks. *Ecol. Lett.* **14**, 75–79. (doi:10.1111/j.1461-0248.2010.01558.x)

116. Christian RR, Thomas CR. 2003 Network analysis of nitrogen inputs and cycling in the Neuse River estuary, North Carolina, USA. *Estuaries* **26**, 815–828. (doi:10.1007/BF02711992)

117. Winfree AT. 1967 Biological rhythms and the behavior of populations of coupled oscillators. *J. Theor. Biol.* **16**, 15–42. (doi:10.1016/0022-5193(67)90051-3)

118. Kuramoto Y. 1975 Self-entrainment of a population of coupled non-linear oscillators. In *Int. Symp. on Mathematical Problems in Theoretical Physics*, 23–29 January 1975, Kyoto University, Kyoto, Japan (ed. H Araki), pp. 420–422. New York, NY: Springer.

119. Rinaldo A, Gatto M, Rodriguez-Iturbe I. 2018 River networks as ecological corridors: a coherent ecohydrological perspective. *Adv. Water Res.* **112**, 27–58. (doi:10.1016/j.advwatres.2017.10.005)

120. Chaput-Bardy A, Alcala N, Secondi J, Vuilleumier S. 2017 Network analysis for species management in rivers networks: application to the Loire river. *Biol. Conserv.* **210**, 26–36. (doi:10.1016/j.biocon.2017.04.003)

121. Hanski I, Ovaskainen O. 2003 Metapopulation theory for fragmented landscapes. *Theor. Popul. Biol.* **64**, 119–127. (doi:10.1016/S0040-5809(03)00022-4)

122. Arumugam R, Lutscher F, Guichard F. 2021 Tracking unstable states: ecosystem dynamics in a changing world. *Oikos* **130**, 525–540. (doi:10.1111/oik.08051)

123. Gilarranz LJ, Hastings A, Bascompte J. 2015 Inferring topology from dynamics in spatial networks. *Theor. Ecol.* **8**, 15–21. (doi:10.1007/s12080-014-0231-y)

124. Luque S, Saura S, Fortin M-J. 2012 Landscape connectivity analysis for conservation: insights from combining new methods with ecological and genetic data. *Landsc. Ecol.* **27**, 153–157. (doi:10.1007/s10980-011-9700-5)

125. Moore JW et al. 2015 Emergent stability in a large, free-flowing watershed. *Ecology* **96**, 340–347. (doi:10.1890/14-0326.1)

126. Terui A, Ishiyama N, Urabe H, Ono S, Finlay JC, Nakamura F. 2018 Metapopulation stability in branching river networks. *Proc. Natl Acad. Sci. USA* **115**, E5963–E5969. (doi:10.1073/pnas.1800060115)

127. Shen-Orr SS, Milo R, Mangan S, Alon U. 2002 Network motifs in the transcriptional regulation network of *Escherichia coli*. *Nat. Genet.* **31**, 64–68. (doi:10.1038/ng881)

128. Zaslaver A, Mayo AE, Rosenberg R, Bashkin P, Sberro H, Tsalyuk M, Surette MG, Alon U. 2004 Just-in-time transcription program in metabolic pathways. *Nat. Genet.* **36**, 486–491. (doi:10.1038/ng1348)

129. Chen KC, Csikasz-Nagy A, Gyorffy B, Val J, Novak B, Tyson JJ. 2000 Kinetic analysis of a molecular model of the budding yeast cell cycle. *Mol. Biol. Cell* **11**, 369–391. (doi:10.1091/mbc.11.1.369)

130. Li F, Long T, Lu Y, Ouyang Q, Tang C. 2004 The yeast cell-cycle network is robustly designed. *Proc. Natl Acad. Sci. USA* **101**, 4781–4786. (doi:10.1073/pnas.0305937101)

131. Davidich MI, Bornholdt S. 2008 Boolean network model predicts cell cycle sequence of fission yeast. *PLoS ONE* **3**, e1672. (doi:10.1371/journal.pone.0001672)

132. Bornholdt S. 2005 Less is more in modeling large genetic networks. *Science* **310**, 449–451. (doi:10.1126/science.1119959)

133. Le Novère N. 2015 Quantitative and logic modelling of molecular and gene networks. *Nat. Rev. Genet.* **16**, 146–158. (doi:10.1038/nrg3885)

134. Hütt M-T, Lesne A. 2020 Gene regulatory networks: dissecting structure and dynamics. In *Systems medicine: integrative, qualitative and computational*

approaches (ed. Olaf Wolkenhauer), pp. 77–85. Amsterdam, The Netherlands: Elsevier.

135. Jeong H, Tombor B, Albert R, Oltvai ZN, Barabási A-L. 2000 The large-scale organization of metabolic networks. *Nature* **407**, 651–654. (doi:10.1038/35036627)

136. Beber ME, Fretter C, Jain S, Sonnenschein N, Müller-Hannemann M, Hütt MT. 2012 Artefacts in statistical analyses of network motifs: general framework and application to metabolic networks. *J. R. Soc. Interface* **9**, 3426–3435. (doi:10.1098/rsif.2012.0490)

137. Hütt M-T. 2014 Understanding genetic variation – the value of systems biology. *Br. J. Clin. Pharmacol.* **77**, 597–605. (doi:10.1111/bcp.12266)

138. Knecht C, Fretter C, Rosenstiel P, Krawczak M, Hütt M-T. 2016 Distinct metabolic network states manifest in the gene expression profiles of pediatric inflammatory bowel disease patients and controls. *Sci. Rep.* **6**, 32584. (doi:10.1038/srep32584)

139. Perrin-Cocon L *et al.* 2021 Lipogenesis and innate immunity in hepatocellular carcinoma cells reprogrammed by an isoenzyme switch of hexokinases. *Commun. Biol.* **1**, 1–15. (doi:10.1101/2020.03.13.973321)

140. Nyczka P, Hütt M-T, Lesne A. 2021 Inferring pattern generators on networks. *Physica A* **566**, 125631. (doi:10.1016/j.physa.2020.125631)

141. Orth JD, Thiele I, Palsson BØ. 2010 What is flux balance analysis? *Nat. Biotechnol.* **28**, 245–248. (doi:10.1038/nbt.1614)

142. O'Brien Edward J, Monk Jonathan M, Palsson Bernhard O. 2015 Using genome-scale models to predict biological capabilities. *Cell* **161**, 971–987. (doi:10.1016/j.cell.2015.05.019)

143. Fell DA. 1992 Metabolic control analysis: a survey of its theoretical and experimental development. *Biochem. J.* **286**, 313–330. (doi:10.1042/bj2860313)

144. Cascante M, Boros LG, Comin-Anduix B, de Atauri P, Centelles JJ, Lee PW-N. 2002 Metabolic control analysis in drug discovery and disease. *Nat. Biotechnol.* **20**, 243–249. (doi:10.1038/nbt0302-243)

145. Oughtred R *et al.* 2019 The BioGRID interaction database: 2019 update. *Nucleic Acids Res.* **47**, 529–541. (doi:10.1093/nar/gky1079)

146. Moreno-Zambrano M, Grimbs S, Ullrich MS, Hütt M-T. 2018 A mathematical model of cocoa bean fermentation. *R. Soc. Open Sci.* **5**, 180964. (doi:10.1098/rsos.180964)

147. Jones EG. 1999 Golgi, cajal and the neuron doctrine. *J. Hist. Neurosci.* **8**, 170–178. (doi:10.1076/jhin.8.2.170.1838)

148. Sporns O, Tononi G, Kötter R. 2005 The human connectome: a structural description of the human brain. *PLoS Comput. Biol.* **1**, e42. (doi:10.1371/journal.pcbi.0010042)

149. Sebastian Seung H. 2011 Towards functional connectomics. *Nature* **471**, 171–172. (doi:10.1038/471170a)

150. Kötter R. 2004 Online retrieval, processing, and visualization of primate connectivity data from the CoCoMac database. *Neuroinformatics* **2**, 127–144. (doi:10.1385/NI:2:2:127)

151. Hagmann P, Cammoun L, Gigandet X, Meuli R, Honey CJ, Wedeen VJ, Sporns O. 2008 Mapping the structural core of human cerebral cortex. *PLoS Biol.* **6**, e159. (doi:10.1371/journal.pbio.0060159)

152. Chiang A-S *et al.* 2011 Three-dimensional reconstruction of brain-wide wiring networks in *Drosophila* at single-cell resolution. *Curr. Biol.* **21**, 1–11. (doi:10.1016/j.cub.2010.11.056)

153. Van Essen DC *et al.* 2012 The human connectome project: a data acquisition perspective. *NeuroImage* **62**, 2222–2231. (doi:10.1016/j.neuroimage.2012.02.018)

154. Oh SW *et al.* 2014 A mesoscale connectome of the mouse brain. *Nature* **508**, 207–214. (doi:10.1038/nature13186)

155. Van den Heuvel MP, Bullmore ET, Sporns O. 2016 Comparative connectomics. *Trends Cogn. Sci.* **20**, 345–361. (doi:10.1016/j.tics.2016.03.001)

156. Helmstaedter M, Briggman KL, Turaga SC, Jain V, Seung HS, Denk W. 2013 Connectomic reconstruction of the inner plexiform layer in the mouse retina. *Nature* **500**, 168–174. (doi:10.1038/nature12346)

157. Markram H *et al.* 2015 Reconstruction and simulation of neocortical microcircuitry. *Cell* **163**, 456–492. (doi:10.1016/j.cell.2015.09.029)

158. Eichler K *et al.* 2017 The complete connectome of a learning and memory centre in an insect brain. *Nature* **548**, 175–182. (doi:10.1038/nature23455)

159. Ercsey-Ravasz M, Markov NT, Lamy C, Van Essen DC, Knoblauch K, Toroczkai Z, Kennedy H. 2013 A predictive network model of cerebral cortical connectivity based on a distance rule. *Neuron* **80**, 184–197. (doi:10.1016/j.neuron.2013.07.036)

160. Cherniak C. 1994 Component placement optimization in the brain. *J. Neurosci.* **14**, 2418–2427. (doi:10.1523/JNEUROSCI.14-04-02418.1994)

161. Chklovskii DB, Schikorski T, Stevens CF. 2002 Wiring optimization in cortical circuits. *Neuron* **34**, 341–347. (doi:10.1016/S0896-6273(02)00679-7)

162. Sporns O, Kötter R. 2004 Motifs in brain networks. *PLoS Biol.* **2**, e369. (doi:10.1371/journal.pbio.0020369)

163. Song S, Sjöström PJ, Reigl M, Nelson S, Chklovskii DB. 2005 Highly nonrandom features of synaptic connectivity in local cortical circuits. *PLoS Biol.* **3**, e68. (doi:10.1371/journal.pbio.0030068)

164. Perin R, Berger TK, Markram H. 2011 A synaptic organizing principle for cortical neuronal groups. *Proc. Natl Acad. Sci. USA* **108**, 5419–5424. (doi:10.1073/pnas.1016051108)

165. Van Den Heuvel MP, Sporns O. 2011 Rich-club organization of the human connectome. *J. Neurosci.* **31**, 15 775–15 786. (doi:10.1523/JNEUROSCI.3539-11.2011)

166. Sizemore AE, Giusti C, Kahn A, Vettel JM, Betzel RF, Bassett DS. 2018 Cliques and cavities in the human connectome. *J. Comput. Neurosci.* **44**, 115–145. (doi:10.1007/s10827-017-0672-6)

167. Bassett DS, Sporns O. 2017 Network neuroscience. *Nat. Neurosci.* **20**, 353–364. (doi:10.1038/nn.4502)

168. Carandini M, Heeger DJ. 2012 Normalization as a canonical neural computation. *Nat. Rev. Neurosci.* **13**, 51–62. (doi:10.1038/nrn3136)

169. Bastos AM, Usrey WM, Adams RA, Mangun GR, Fries P, Friston KJ. 2012 Canonical microcircuits for predictive coding. *Neuron* **76**, 695–711. (doi:10.1016/j.neuron.2012.10.038)

170. Fornito A, Zalesky A, Breakspear M. 2015 The connectomics of brain disorders. *Nat. Rev. Neurosci.* **16**, 159–172. (doi:10.1038/nrn3901)

171. Marr D, Poggio T. 1976 *From understanding computation to understanding neural circuitry*. Cambridge, MA: MIT.

172. Fox MD, Raichle ME. 2007 Spontaneous fluctuations in brain activity observed with functional magnetic resonance imaging. *Nat. Rev. Neurosci.* **8**, 700–711. (doi:10.1038/nrn2201)

173. Buzsaki G. 2006 *Rhythms of the brain*. Oxford, UK: Oxford University Press.

174. Wang X-J. 2010 Neurophysiological and computational principles of cortical rhythms in cognition. *Physiol. Rev.* **90**, 1195–1268. (doi:10.1152/physrev.00035.2008)

175. Varela F, Lachaux J-P, Rodriguez E, Martinerie J. 2001 The brainweb: phase synchronization and large-scale integration. *Nat. Rev. Neurosci.* **2**, 229–239. (doi:10.1038/35067550)

176. Brunel N, Wang X-J. 2003 What determines the frequency of fast network oscillations with irregular neural discharges? I. Synaptic dynamics and excitation–inhibition balance. *J. Neurophysiol.* **90**, 415–430. (doi:10.1152/jn.01095.2002)

177. Fries P. 2015 Rhythms for cognition: communication through coherence. *Neuron* **88**, 220–235. (doi:10.1016/j.neuron.2015.09.034)

178. Roelfsema PR, Engel AK, König P, Singer W. 1997 Visuomotor integration is associated with zero time-lag synchronization among cortical areas. *Nature* **385**, 157–161. (doi:10.1038/385157a0)

179. Fries P, Reynolds JH, Rorie AE, Desimone R. 2001 Modulation of oscillatory neuronal synchronization by selective visual attention. *Science* **291**, 1560–1563. (doi:10.1126/science.1055465)

180. Canolty RT, Knight RT. 2010 The functional role of cross-frequency coupling. *Trends Cogn. Sci.* **14**, 506–515. (doi:10.1016/j.tics.2010.09.001)

181. Uhlhaas PJ, Singer W. 2012 Neuronal dynamics and neuropsychiatric disorders: toward a translational paradigm for dysfunctional large-scale networks. *Neuron* **75**, 963–980. (doi:10.1016/j.neuron.2012.09.004)

182. Friston KJ. 2011 Functional and effective connectivity: a review. *Brain Connectivity* **1**, 13–36. (doi:10.1089/brain.2011.0008)

183. Liu L, Ioannides AA. 2006 Spatiotemporal dynamics and connectivity pattern differences between centrally and peripherally presented faces. *NeuroImage* **31**, 1726–1740. (doi:10.1016/j.neuroimage.2006.02.009)

184. Abeles M. 1991 *Corticonics: neural circuits of the cerebral cortex*. Cambridge, UK: Cambridge University Press.

185. Ikegaya Y, Aaron G, Cossart R, Aronov D, Lampl I, Ferster D, Yuste R. 2004 Synfire chains and cortical songs: temporal modules of cortical activity. *Science* **304**, 559–564. (doi:10.1126/science.1093173)

186. Mitra A, Snyder AZ, Blazey T, Raichle ME. 2015 Lag threads organize the brain's intrinsic activity. *Proc. Natl Acad. Sci. USA* **112**, E2235–E2244. (doi:10.1073/pnas.1503960112)

187. Battaglia D, Witt A, Wolf F, Geisel T. 2012 Dynamic effective connectivity of inter-areal brain circuits. *PLoS Comput. Biol.* **8**, e1002438. (doi:10.1371/journal.pcbi.1002438)

188. Bastos AM, Vezoli J, Fries P. 2015 Communication through coherence with inter-areal delays. *Curr. Opin Neurobiol.* **31**, 173–180. (doi:10.1016/j.conb.2014.11.001)

189. Carlos F-LP, Ubirakitan M-M, Rodrigues MCA, Aguilar-Domingo M, Herrera-Gutiérrez E, Gómez-Amor J, Copelli M, Carelli PV, Matias FS. 2020 Anticipated synchronization in human EEG data: unidirectional causality with negative phase lag. *Phys. Rev. E* **102**, 032216. (doi:10.1103/PhysRevE.102.032216)

190. Deschle N, Daffertshofer A, Battaglia D, Martens EA. 2019 Directed flow of information in chimera states. *Front. Appl. Math. Stat.* **5**, 28. (doi:10.3389/fams.2019.00028)

191. Brovelli A, Ding M, Ledberg A, Chen Y, Nakamura R, Bressler SL. 2004 Beta oscillations in a large-scale sensorimotor cortical network: directional influences revealed by granger causality. *Proc. Natl Acad. Sci. USA* **101**, 9849–9854. (doi:10.1073/pnas.0308538101)

192. Ding M, Chen Y, Bressler SL. 2006 Granger causality: basic theory and application to neuroscience. In *Handbook of Time Series Analysis: Recent Theoretical Developments and Applications* (eds B Schelter, M Winterhalder, J Timmer), pp. 437–460. Weinheim, Germany: Wiley-VCH.

193. Gregoriou GG, Gotts SJ, Zhou H, Desimone R. 2009 High-frequency, long-range coupling between prefrontal and visual cortex during attention. *Science* **324**, 1207–1210. (doi:10.1126/science.1171402)

194. Dhamala M, Rangarajan G, Ding M. 2008 Estimating Granger causality from Fourier and wavelet transforms of time series data. *Phys. Rev. Lett.* **100**, 018701. (doi:10.1103/PhysRevLett.100.018701)

195. Bastos AM, Vezoli Julien, Bosman CA, Schoffelen J-M, Oostenveld R, Dowdall JR, De Weerd P, Kennedy H, Fries P. 2015 Visual areas exert feedforward and feedback influences through distinct frequency channels. *Neuron* **85**, 390–401. (doi:10.1016/j.neuron.2014.12.018)

196. Michalareas G, Vezoli J, Van Pelt S, Schoffelen J-M, Kennedy H, Fries P. 2016 Alpha-beta and gamma rhythms subserve feedback and feedforward influences among human visual cortical areas. *Neuron* **89**, 384–397. (doi:10.1016/j.neuron.2015.12.018)

197. Holme P, Saramäki J. 2012 Temporal networks. *Phys. Rep.* **519**, 97–125. (doi:10.1016/j.physrep.2012.03.001)

198. Calhoun VD, Miller R, Pearlson G, Adalı T. 2014 The chronnectome: time-varying connectivity networks as the next frontier in fMRI data discovery. *Neuron* **84**, 262–274. (doi:10.1016/j.neuron.2014.10.015)

199. Ioannides AA. 2007 Dynamic functional connectivity. *Curr. Opin Neurobiol.* **17**, 161–170. (doi:10.1016/j.conb.2007.03.008)

200. Brovelli A, Badier J-M, Bonini F, Bartolomei F, Coulon O, Auzias G. 2017 Dynamic reconfiguration of visuomotor-related functional connectivity networks. *J. Neurosci.* **37**, 839–853. (doi:10.1523/JNEUROSCI.1672-16.2016)

201. Braun U et al. 2015 Dynamic reconfiguration of frontal brain networks during executive cognition in humans. *Proc. Natl Acad. Sci. USA* **112**, 11 678–11 683. (doi:10.1073/pnas.1422487112)

202. Lombardo D et al. 2020 Modular slowing of resting-state dynamic functional connectivity as a marker of cognitive dysfunction induced by sleep deprivation. *NeuroImage* **222**, 117155. (doi:10.1016/j.neuroimage.2020.117155)

203. Pedreschi N, Bernard C, Clawson W, Quilichini P, Barrat A, Battaglia D. 2020 Dynamic core-periphery structure of information sharing networks in entorhinal cortex and hippocampus. *Netw. Neurosci.* **4**, 946–975. (doi:10.1162/netn_a_00142)

204. Clawson W, Vicente AF, Ferraris M, Bernard C, Battaglia D, Quilichini PP. 2019 Computing hubs in the hippocampus and cortex. *Sci. Adv.* **5**, eaax4843. (doi:10.1126/sciadv.aax4843)

205. Kirst C, Timme M, Battaglia D. 2016 Dynamic information routing in complex networks. *Nat. Commun.* **7**, 1–9. (doi:10.1038/ncomms11061)

206. Battaglia D. 2014 Function follows dynamics: state-dependency of directed functional influences. In *Directed information measures in neuroscience*, (eds M Wibral, R Vicente, J Lizier) pp. 111–135. New York, NY: Springer. (doi:10.1007/978-3-642-54474-3_5)

207. Kopell NJ, Gritton HJ, Whittington MA, Kramer MA. 2014 Beyond the connectome: the dynome. *Neuron* **83**, 1319–1328. (doi:10.1016/j.neuron.2014.08.016)

208. Ghosh A, Rho Y, McIntosh AR, Kötter R, Jirsa VK. 2008 Noise during rest enables the exploration of the brain's dynamic repertoire. *PLoS Comput. Biol.* **4**, e1000196. (doi:10.1371/journal.pcbi.1000196)

209. Marder E, Goaillard J-M. 2006 Variability, compensation and homeostasis in neuron and network function. *Nat. Rev. Neurosci.* **7**, 563–574. (doi:10.1038/nrn1949)

210. Marrelec Guillaume, Messé Arnaud, Giron Alain, Rudrauf David. 2016 Functional connectivity's degenerate view of brain computation. *PLoS Comput. Biol.* **12**, e1005031. (doi:10.1371/journal.pcbi.1005031)

211. Stetter O, Battaglia D, Soriano J, Geisel T. 2012 Model-free reconstruction of excitatory neuronal connectivity from calcium imaging signals. *PLoS Comput. Biol.* **8**, e1002653. (doi:10.1371/journal.pcbi.1002653)

212. Honey CJ, Kötter R, Breakspear M, Sporns O. 2007 Network structure of cerebral cortex shapes functional connectivity on multiple time scales. *Proc. Natl Acad. Sci. USA* **104**, 10 240–10 245. (doi:10.1073/pnas.0701519104)

213. Deco G, Jirsa VK, McIntosh AR. 2011 Emerging concepts for the dynamical organization of resting-state activity in the brain. *Nat. Rev. Neurosci.* **12**, 43–56. (doi:10.1038/nrn2961)

214. Atasoy S, Donnelly I, Pearson J. 2016 Human brain networks function in connectome-specific harmonic waves. *Nat. Commun.* **7**, 1–10. (doi:10.1038/ncomms10340)

215. Deco G, Senden M, Jirsa V. 2012 How anatomy shapes dynamics: a semi-analytical study of the brain at rest by a simple spin model. *Front. Comput. Neurosci.* **6**, 68. (doi:10.3389/fncom.2012.00068)

216. Papadopoulos L, Lynn CW, Battaglia D, Bassett DS. 2020 Relations between large-scale brain connectivity and effects of regional stimulation depend on collective dynamical state. *PLoS Comput. Biol.* **16**, e1008144. (doi:10.1371/journal.pcbi.1008144)

217. Hansen ECA, Battaglia D, Spiegler A, Deco G, Jirsa VK. 2015 Functional connectivity dynamics: modeling the switching behavior of the resting state. *NeuroImage* **105**, 525–535. (doi:10.1016/j.neuroimage.2014.11.001)

218. Folke C, Biggs R, Norström AV, Reyers B, Rockström J. 2016 Social-ecological resilience and biosphere-based sustainability science. *Ecol. Soc.* **21**, 41. (doi:10.5751/ES-08748-210341)

219. Martinez-Alier J. 1987 *Ecological economics: energy, environment and society*. Oxford, UK: Basil Blackwell.

220. Bodin Ö, Prell C. 2011 *Social networks and natural resource management: uncovering the social fabric of environmental governance*. Cambridge, UK: Cambridge University Press.

221. Barnes ML, Bodin Ö, Guerrero AM, McAllister RRJ, Alexander SM, Robins G. 2017 The social structural foundations of adaptation and transformation in social–ecological systems. *Ecol. Soc.* **22**, 16. (doi:10.5751/ES-09769-220416)

222. Bodin Ö, Tengö M. 2012 Disentangling intangible social–ecological systems. *Global Environ. Change* **22**, 430–439. (doi:10.1016/j.gloenvcha.2012.01.005)

223. Sayles JS, Garcia MM, Hamilton M, Alexander SM, Baggio JA, Fischer AP, Ingold K, Meredith GR, Pittman J. 2019 Social-ecological network analysis for sustainability sciences: a systematic review and innovative research agenda for the future. *Environ. Res. Lett.* **14**, 093003. (doi:10.1088/1748-9326/ab2619)

224. Prell C, Sun L, Feng K, He J, Hubacek K. 2017 Uncovering the spatially distant feedback loops of global trade: a network and input–output approach. *Sci. Total Environ.* **586**, 401–408. (doi:10.1016/j.scitotenv.2016.11.202)

225. Wang P, Robins G, Pattison P, Lazega E. 2013 Exponential random graph models for multilevel networks. *Soc. Netw.* **35**, 96–115. (doi:10.1016/j.socnet.2013.01.004)

226. Sáenz de Tejada R. 2007 Democracias de posguerra en Centroamérica : política, pobreza y desigualdad en Nicaragua, El Salvador y Guatemala (1979–2005). PhD thesis, Facultad Latinoamericana de Ciencias Sociales Sede, Ecuador.

227. Luhmann N. 1984 *Soziale systeme: grundriss einer allgemeinen theorie*. Frankfurt am Main, Germany: Suhrkamp.

228. Scott J. 2013 Social network analysis, 3rd edn, Los Angeles, CA: Sage.

229. Jansen D. 1999 *Einführung in die netzwerkanalyse: Grundlagen, methoden, anwendung*. Operladen, Germany: Leske & Budrich.

230. Stadtfeld C, Block P. 2017 Interactions, actors, and time: dynamic network actor models for relational events. *Sociol. Sci.* **4**, 318–352. (doi:10. 15195/v4.a14)

231. Fath BD, Scharler UM, Ulanowicz RE, Hannon B. 2007 Ecological network analysis: network construction. *Ecol. Modell.* **208**, 49–55. (doi:10. 1016/j.ecolmodel.2007.04.029)

232. Ulanowicz RE. 1983 Identifying the structure of cycling in ecosystems. *Math. Biosci.* **65**, 219–237. (doi:10.1016/0025-5564(83)90063-9)

233. Leontief WW. 1936 Quantitative Input and Output relations in the economic systems of the United States. *Rev. Econ. Stat.* **18**, 105–125. (doi:10.2307/1927837)

234. Miller RE, Blair PD. 2009 *Input–output analysis: foundations and extensions*. Cambridge, UK: Cambridge University Press.

235. Chen S, Chen B. 2015 Urban energy consumption: different insights from energy flow analysis, input–output analysis and ecological network analysis. *Appl. Energy* **138**, 99–107. (doi:10.1016/j.apenergy. 2014.10.055)

236. Fath BD, Patten BC. 1999 Quantifying resource homogenization using network flow analysis. *Ecol. Modell* **123**, 193–205. (doi:10.1016/S0304-3800(99)00130-1)

237. Fath BD. 2004 Distributed control in ecological networks. *Ecol. Modell.* **179**, 235–245. (doi:10. 1016/j.ecolmodel.2004.06.007)

238. Hall CAS, Balogh S, Murphy DJR. 2009 What is the minimum EROI that a sustainable society must have? *Energies* **2**, 25–47. (doi:10.3390/en20100025)

239. Georgescu-Roegen N. 1975 Energy and economic myths. *South. Econ. J.* **41**, 347–381. (doi:10.2307/1056148)

240. Tainter J. 1988 *The collapse of complex societies*. Cambridge, UK: Cambridge University Press.

241. Odum HT. 2007 *Environment, power, and society for the twenty-first century: the hierarchy of energy*. New York, NY: Columbia University Press.

242. Hornborg A. 1998 Towards an ecological theory of unequal exchange: articulating world system theory and ecological economics. *Ecol. Econ.* **25**, 127–136. (doi:10.1016/S0921-8009(97)00100-6)

243. Barnes ML, Bodin Ö, McClanahan TR, Kittinger JN, Hoey AS, Gaoue OG, Graham NAJ. 2019 Social–ecological alignment and ecological conditions in coral reefs. *Nat. Commun.* **10**, 1–10. (doi:10.1038/s41467-019-09994-1)

244. Janssen MA, Ostrom E. 2006 Resilience, vulnerability, and adaptation: a cross-cutting theme of the international human dimensions programme on global environmental change. *Glob. Environ. Change* **16**, 237–239. (doi:10.1016/j.gloenvcha. 2006.04.003)

245. Sayles JS, Baggio JA. 2017 Social–ecological network analysis of scale mismatches in estuary watershed restoration. *Proc. Natl Acad. Sci. USA* **114**, E1776–E1785. (doi:10.1073/pnas.1604405114)

246. Schlüter M, Haider LJ, Lade SJ, Lindkvist E, Martin R, Orach K, Wijermans N, Folke C. 2019 Capturing emergent phenomena in social-ecological systems. *Ecol. Soc.* **24**, 11. (doi:10.5751/ES-11012-240311).

247. Bodin Ö, Mancilla García M, Robins G. 2020 Reconciling conflict and cooperation in environmental governance: a social network perspective. *Annu. Rev. Environ. Resourc.* **45**, 471–495. (doi:10.1146/annurev-environ-011020-064352)

248. Nelson DR, Adger WN, Brown K. 2007 Adaptation to environmental change: contributions of a resilience framework. *Annu. Rev. Environ. Resourc.* **32**, 395–419. (doi:10.1146/annurev.energy.32.051807. 090348)

249. Newman L, Dale A. 2005 Network structure, diversity, and proactive resilience building: a response to Tompkins and Adger. *Ecol. Soc.* **10**, R2. (doi:10.5751/ES-01396-1001r02)

250. Folke C, Carpenter SR, Walker B, Scheffer M, Chapin T, Rockström J. 2010 Resilience thinking: integrating resilience, adaptability and transformability. *Ecol. Soc.* **15**, 20. (doi:10.5751/ES-03610-150420)

251. Walker B, Holling CS, Carpenter SR, Kinzig A. 2004 Resilience, adaptability and transformability in social–ecological systems. *Ecol. Soc.* **9**, 5. (doi:10. 5751/ES-00650-090205)

252. Rocha CD, Tezel A, Talebi S, Koskela L. 2018 Product modularity, tolerance management, and visual management: potential synergies. In *Proc. of the 26th Annual Conf. of the Int. Group for Lean Construction, Chennai, India*, (ed. VA González) pp. 18–20. (doi:10.24928/2018/0482)

253. Kimmich C. 2013 Linking action situations: coordination, conflicts, and evolution in electricity provision for irrigation in Andhra Pradesh, India. *Ecol. Econ.* **90**, 150–158. (doi:10.1016/j.ecolecon. 2013.03.017)

254. Hughes G, Desantis A, Waszak F. 2013 Attenuation of auditory N1, results from identity-specific action-effect prediction. *Eur. J. Neurosci.* **37**, 1152–1158. (doi:10.1111/ejn.12120)

255. Liu L, Oza S, Hogan D, Perin J, Rudan I, Lawn JE, Cousens S, Mathers C, Black RE. 2015 Global, regional, and national causes of child mortality in 2000–13, with projections to inform post-2015 priorities: an updated systematic analysis. *Lancet* **385**, 430–440. (doi:10.1016/S0140-6736(14)61698-6)

256. Leontief W *et al.* 1974 Environmental repercussions and the economic structure: an input–output approach: a reply. *Rev. Econ. Stat.* **56**, 109–110. (doi:10.2307/1927535)

257. Buzsáki G, Mizuseki K. 2014 The log-dynamic brain: how skewed distributions affect network operations. *Nat. Rev. Neurosci.* **15**, 264–278. (doi:10.1038/nrn3687)

258. Gallos LK, Song C, Havlin S, Makse HA. 2007 Scaling theory of transport in complex biological networks. *Proc. Natl Acad. Sci. USA* **104**, 7746–7751. (doi:10.1073/pnas.0700250104)

259. Lorenz EN. 1963 Deterministic nonperiodic flow. *J. Atmos. Sci.* **20**, 130–141. (doi:10.1175/1520-0469(1963)020<0130:DNF>2.0.CO;2)

260. Josić K, Wayne CE. 2000 Dynamics of a ring of diffusively coupled Lorenz oscillators. *J. Stat. Phys.* **98**, 1–30. (doi:10.1023/A:1018600203530)

261. Rössler OE. 1976 An equation for continuous chaos. *Phys. Lett. A* **57**, 397–398. (doi:10.1016/0375-9601(76)90101-8)

262. Majhi S, Ghosh D, Kurths J. 2019 Emergence of synchronization in multiplex networks of mobile Rössler oscillators. *Phys. Rev. E* **99**, 012308. (doi:10. 1103/PhysRevE.99.012308)

263. Selivanov AA, Lehnert J, Dahms T, Hövel P, Fradkov AL, Schöll E. 2012 Adaptive synchronization in delay-coupled networks of Stuart-Landau oscillators. *Phys. Rev. E* **85**, 016201. (doi:10.1103/PhysRevE.85.016201)

264. Panteley E, Loria A, El Ati A. 2015 On the stability and robustness of Stuart-Landau oscillators. *IFAC-PapersOnLine* **48**, 645–650. (doi:10.1016/j.ifacol. 2015.09.260)

265. Minati L, Chiesa P, Tabarelli D, D'Incerti L, Jovich J. 2015 Synchronization, non-linear dynamics and low-frequency fluctuations: analogy between spontaneous brain activity and networked single-transistor chaotic oscillators. *Chaos* **25**, 033107. (doi:10.1063/1.4914938)

266. Minati L, Ito H, Perinelli A, Ricci L, Faes L, Yoshimura N, Koike Y, Frasca M. 2019 Connectivity influences on nonlinear dynamics in weakly-synchronized networks: insights from Rössler systems, electronic chaotic oscillators, model and biological neurons. *IEEE Access* **7**, 174 793–174 821. (doi:10.1109/ACCESS.2019. 2957014)

267. Noël P-A, Brummitt CD, D'Souza RM. 2014 Bottom-up model of self-organized criticality on networks. *Phys. Rev. E* **89**, 012807. (doi:10.1103/PhysRevE.89. 012807)

268. Giuraniuc CV, Hatchett JPL, Indekeu JO, Leone M, Pérez Castillo I, Van Schaeybroeck B, Vanderzande C. 2006 Criticality on networks with topology-dependent interactions. *Phys. Rev. E* **74**, 036108. (doi:10.1103/PhysRevE.74.036108)

269. Rubinov M, Sporns O, Thivierge J-P, Breakspear M. 2011 Neurobiologically realistic determinants of self-organized criticality in networks of spiking neurons. *PLoS Comput. Biol.* **7**, e1002038. (doi:10. 1371/journal.pcbi.1002038)

270. Moretti P, Muñoz MA. 2013 Griffiths phases and the stretching of criticality in brain networks. *Nat. Commun.* **4**, 1–10. (doi:10.1038/ncomms3521)

271. Hilgetag CC, Hütt M-T. 2014 Hierarchical modular brain connectivity is a stretch for criticality.

Trends Cogn. Sci. **18**, 114–115. (doi:10.1016/j.tics.2013.10.016)

272. Yeung MKS, Strogatz SH. 1999 Time delay in the Kuramoto model of coupled oscillators. *Phys. Rev. Lett.* **82**, 648. (doi:10.1103/PhysRevLett.82.648)

273. Klinshov VV, Nekorkin VI. 2013 Synchronization of delay-coupled oscillator networks. *Phys. Usp.* **56**, 1217. (doi:10.3367/UFNe.0183.201312c.1323)

274. Gil S, Mikhailov AS. 2009 Networks on the edge of chaos: global feedback control of turbulence in oscillator networks. *Phys. Rev. E* **79**, 026219. (doi:10.1103/PhysRevE.79.026219)

275. Dhamala M, Jirsa VK, Ding M. 2004 Enhancement of neural synchrony by time delay. *Phys. Rev. Lett.* **92**, 074104. (doi:10.1103/PhysRevLett.92.074104)

276. Deco G, Jirsa V, McIntosh AR, Sporns O, Kötter R. 2009 Key role of coupling, delay, and noise in resting brain fluctuations. *Proc. Natl Acad. Sci. USA* **106**, 10 302–10 307. (doi:10.1073/pnas.0901831106)

277. Ravasz E, Somera AL, Mongru DA, Oltvai ZN, Barabási A-L. 2002 Hierarchical organization of modularity in metabolic networks. *Science* **297**, 1551–1555. (doi:10.1126/science.1073374)

278. Watts DJ, Strogatz SH. 1998 Collective dynamics of 'small-world' networks. *Nature* **393**, 440. (doi:10.1038/30918)

279. Erdős P, Rényi A. 1959 On random graphs. *Publ. Math. (Debrecen)* **6**, 290.

280. Barabási A-L, Albert R. 1999 Emergence of scaling in random networks. *Science* **286**, 509–512. (doi:10.1126/science.286.5439.509)

281. Maslov S, Sneppen K. 2002 Specificity and stability in topology of protein networks. *Science* **296**, 910–913. (doi:10.1126/science.1065103)

282. Drossel B, Schwabl F. 1992 Self-organized critical forest-fire model. *Phys. Rev. Lett.* **69**, 1629. (doi:10.1103/PhysRevLett.69.1629)

283. Müller-Linow M, Marr C, Hütt M-T. 2006 Topology regulates the distribution pattern of excitations in excitable dynamics on graphs. *Phys. Rev. E* **74**, 016112. (doi:10.1103/PhysRevE.74.016112)

284. Acebrón JA, Bonilla LL, Vicente CJP, Ritort F, Spigler R. 2005 The Kuramoto model: a simple paradigm for synchronization phenomena. *Rev. Mod. Phys.* **77**, 137. (doi:10.1103/RevModPhys.77.137)

285. May RM. 1976 Simple mathematical models with very complicated dynamics. *Nature* **261**, 459–467. (doi:10.1038/261459a0)

286. Vadivasova TE, Strelkova GI, Bogomolov SA, Anishchenko VS. 2016 Correlation analysis of the coherence–incoherence transition in a ring of nonlocally coupled logistic maps. *Chaos* **26**, 093108. (doi:10.1063/1.4962647)

287. Rubinov M, Sporns O, van Leeuwen C, Breakspear M. 2009 Symbiotic relationship between brain structure and dynamics. *BMC Neurosci.* **10**, 1–18. (doi:10.1186/1471-2202-10-55)

288. FitzHugh R. 1961 Impulses and physiological states in theoretical models of nerve membrane. *Biophys. J.* **1**, 445–466. (doi:10.1016/S0006-3495(61)86902-6)

289. Nagumo J, Arimoto S, Yoshizawa S. 1962 An active pulse transmission line simulating nerve axon. *Proc. IRE* **50**, 2061–2070. (doi:10.1109/JRPROC.1962.288235)

290. Grace M, Hütt M-T. 2013 Predictability of spatio-temporal patterns in a lattice of coupled Fitzhugh–Nagumo oscillators. *J. R. Soc. Interface* **10**, 20121016. (doi:10.1098/rsif.2012.1016)